NASA Technical Memorandum 85653

A Rate-Controlled Teleoperator Task With Simulated Transport Delays

Jack E. Pennington

SEPTEMBER 1983

25th Anniversary
1958-1983

NASA

NASA Technical Memorandum 85653

A Rate-Controlled Teleoperator Task With Simulated Transport Delays

Jack E. Pennington
Langley Research Center
Hampton, Virginia

National Aeronautics
and Space Administration

**Scientific and Technical
Information Branch**

1983

SUMMARY

The capability for simulating a teleoperator/robotic system is being developed to support research and technology programs related to remote space operations. A preliminary version of this simulation has been used to examine the effects of control modes, a visual proximity cue, and time delays on the manual control of a probe-in-hole alignment task using a simulated five-degree-of-freedom manipulator and computer-generated visual displays.

Three visual displays were simulated. Two displays represented television pictures taken from movable cameras, the locations of which could be controlled by the subjects. The third display represented a television (TV) picture from a fixed camera looking along the axis of the probe. The subjects preferred to position the two movable cameras to provide front and side orthographic views. The subjects had little apparent difficulty in assimilating the visual information, despite having to select the view to be presented on the single TV monitor.

Two control modes were simulated: joint-by-joint proportional-rate control and resolved-rate control with discrete translational rates and proportional rotational rates. Proportional rates were commanded by using a two-axis rotational hand controller and a joint-axis switch matrix. The time required to complete the simulated task was more than three times longer using joint-by-joint control than when using resolved-rate control, and alignment errors were significantly larger when using joint-by-joint control.

The proximity display was a cross icon superimposed on the probe TV picture, with the length of each arm of the cross proportional to the distance from the simulated task board. Rotational errors were indicated by unequal arm lengths. Thus, the proximity-sensor display enabled subjects to separate rotational errors from displacement (translation) errors. Therefore, when the proximity display was used with resolved-rate control, the simulation task was trivial.

Time delays up to 2 sec were simulated. For time delays of 0.25 sec and longer, subjects replaced continuous control with a move-and-wait control strategy. Displaying a cue that the input had been received was helpful for longer time delays. The time required to perform the simulation task increased linearly with time delay, but time delays had no effect on alignment accuracy.

Based on the results of this simulation, several future studies are recommended.

INTRODUCTION

The Langley Research Center is supporting the development of teleoperator and robotics technology that will be required for remote space operations such as satellite servicing, inspection, recovery, fuel transfer, and construction. This research and technology program makes use of (1) a Teleoperator/Robotic Systems Simulation (TRSS) which will model in software actual or conceptual teleoperator/robotic systems; (2) an Intelligent Systems Research Laboratory (ISRL) having a network of distributed microcomputers and minicomputers interfaced to vision systems, speech synthesis and recognition systems, and dual six-degree-of-freedom manipulators equipped with end effectors having touch, force, torque, and proximity sensors; and (3) a reconfigurable control station with multipurpose displays and controllers with which man can interface with the simulation and/or the laboratory. Presently, each of these facilities is under development and in various stages of completion. Capabilities will evolve and improve during the course of the research programs.

This report describes the initial teleoperator simulation which examined the effects of control modes, a proximity-display method, and time delays for a probe-in-hole alignment task using a simulated five-degree-of-freedom manipulator.

SYMBOLS

Values are given in SI Units and, where considered useful, also in U.S. Customary Units. Measurements and calculations were made in U.S. Customary Units.

J	5 × 5 Jacobian matrix
J_3	3 × 3 submatrix of J
K	empirical constant used to limit arm extension
L_1, L_2	length of manipulator upper arm and lower arm, respectively, cm
T	3 × 3 matrix transforming velocity commands from end-effector coordinates to X,Y,Z system
T_J	completion time using joint-by-joint control
T_R	completion time using resolved-rate control
Δt	time delay, sec
X,Y,Z	components of orthogonal coordinate system located at manipulator shoulder, cm
$\dot{X}_C, \dot{Y}_C, \dot{Z}_C$	components of end-effector velocity commanded from cockpit, cm/sec
α	$= \theta_1 + \theta_2 + \theta_3$, deg
$\theta_1, \theta_2, \theta_3$	angle-of-pitch rotation at manipulator shoulder, elbow, and wrist, respectively, deg
$\dot{\theta}$	$= \dot{\theta}_1 + \dot{\theta}_2 + \dot{\theta}_3$
$\dot{\theta}_C$	pitch rate of end effector commanded from cockpit, deg/sec
σ	standard deviation, cm or deg
χ^2	chi-square distribution
ψ_1, ψ_3	angle-of-yaw rotation at manipulator waist and wrist, respectively, deg

$\dot{\phi}$ $= \dot{\phi}_1 + \dot{\phi}_3$

$\dot{\phi}_c$ yaw rate of end effector commanded from cockpit, deg/sec

A dot over a symbol indicates differentiation with respect to time.

DESCRIPTION OF SIMULATION

The teleoperator/robotics simulation is programmed on a CDC[1] CYBER 175 computer operating in real time at 32 iterations per second, which is interfaced to an ADAGE GPS/340 graphics system and a single-place general-purpose cockpit. Manipulator equations, relative geometry, and data recording are handled by the CYBER 175. The ADAGE draws high-speed, monochrome vector (stroke) displays by using data from the CYBER. The vector display is converted to a 525-line television (raster) format by a vidicon camera facing the ADAGE-display cathode-ray tube (CRT). Figure 1 shows an ADAGE drawing of the simulated manipulator.

Simulated Manipulator and Task Board

The simulation models a five-degree-of-freedom manipulator having yaw at the waist, pitch at the shoulder, pitch at the elbow, and pitch and yaw at the wrist. Figure 2 illustrates the manipulator configuration.

Each axis is assumed to respond as a second-order linear servo system; the damping ratio is 0.7 in all axes; and the natural frequency is 5 rad/sec in the first two joints (waist and shoulder) and 10 rad/sec in the other three joints (elbow and wrist). The upper and lower arms are each 43 cm (17 in.) long, and the probe attached to the wrist is 15 cm (6 in.) long.

The order of rotation and the arm lengths are representative of the UNIMATE PUMA[2] manipulators installed in the ISRL. However, the image of the simulated manipulator is more representative of the Protoflight Manipulator Arm (PFMA) at the Marshall Space Flight Center. (See ref. 1.)

The simulation also models a 61-cm^2 (2-ft^2) planar task board containing five "holes." (See fig. 3.) The subject's task was to align the probe accurately with the center of each hole. Forces and moments at contact and compliance were not modeled, but probe angular misalignment and the displacement of the tip of the probe with respect to the center of the hole were computed.

Simulator Cockpit

Figure 4 is a photograph of the simulator cockpit. This general-purpose cockpit is equipped with aircraft instruments, a three-axis proportional hand controller, a

---

[1]CDC: Registered trademark of Control Data Corporation.
[2]UNIMATE PUMA: Registered trademark of Unimation, Inc.

throttle lever, mode-select switches, and indicator lights. This simulation used the following equipment:

(1) A 33-cm (13-in.) black-and-white television (TV) monitor mounted at the top center of the cockpit

(2) A three-axis hand controller for yaw and pitch commands

(3) A speed-brake switch located on the throttle lever for fore and aft translation commands

(4) A mode-select switch panel on the left side of the instrument panel. Mode-select options are described in the next section.

(5) Two three-position center-loaded toggle switches, located below the mode-select panel, for up-down and right-left translation commands

(6) Two lights, below the toggle switches, to indicate when the computer was limiting manipulator motion as the arm neared full extension

(7) A light directly below the TV monitor to indicate satisfactory probe alignment at contact

The other switches, indicators, and instruments in the simulator cockpit were not used.

DISPLAY AND CONTROL MODES

The display options and the control modes were selected by using the mode-select panel located on the left side of the instrument panel. This 4 × 4 matrix of back-lit switches is illustrated in figure 5. Only 10 switches were used in the simulation.

Camera and Display Control

Three TV cameras were simulated: camera 1, camera 2, and the probe TV camera. Three switches in the first column of the mode-select panel were used to select the view to be displayed on the monitor. Cameras 1 and 2 could be moved by the operator. The probe TV camera was fixed, looking along the axis of the probe. A symbol representing the line of sight (axis of the probe) was superimposed on the probe-TV visual scene. Control of cameras 1 and 2 was enabled by selecting the camera with one of the switches in the first (left) column of the mode-select panel, and then selecting the "TV"-control-mode switch in the second column. In this mode, the three translation (on-off) switches commanded translation of the TV camera (up-down, right-left, and fore-aft) with respect to TV-camera axes. The simulated TV camera would translate at 1 m/sec (39 in/sec) as long as a translation command was applied. The TV-camera pan (yaw) and tilt (pitch) were commanded by the rotational controller at a maximum rate of 15 deg/sec. Controller roll input had no effect. Initially, one camera was at a location above the manipulator and task board, and the other camera was looking in from the side.

The "Reset TV" switch was included as a camera-control option because, initially, there was concern that subjects might have trouble assimilating the visual information or that they might move a TV camera to an undesirable or confusing location; thus, some means was needed for the subjects to restore a familiar visual environment. Pressing the "Reset TV" switch would cause the selected TV camera to return to its initial location. However, when testing began it was apparent that the visual scene did not confuse or disorient the subjects. Thus, the "Reset TV" option, although available, was not needed or used.

Proximity-Sensor Display

The availability of a simulated proximity display was one of the parameters in the study. Previous studies at the Jet Propulsion Laboratory (JPL) (refs. 2 and 3) have shown that proximity sensors can be incorporated in an end effector and can supply useful range and alignment information. For the simulation, it was assumed that four proximity sensors were located around the probe to provide range information within 15 cm (6 in.) of the task board. The simulated sensor outputs were represented by four bars located around the probe line-of-sight symbol. When the probe was perpendicular to the task board, the display would be a cross, with size proportional to range. Figure 6 shows the proximity display indicating the probe rotated (yawed) to the right. The proximity display was available only with the "Probe TV" mode selected and the "Proximity display" switch on. (See fig. 5.)

Input-Confirmation Display

A small arrow was displayed in the lower right corner of the TV monitor during control inputs. This display (fig. 7) confirmed that the computer had received the input. A double arrow indicated a translation input, and a single arrow in the direction of motion indicated a rotational input. The arrow also provided an indication of the duration of the control input. It was not subject to the transport delays in the visual scene. The subjects felt that the indicator was most useful with the longer time delays for confirming that the computer had received the command and that a result would eventually appear. Although the input-confirmation display was probably not necessary when there was no transport delay, the display was not distracting and, therefore, it was used throughout the study.

Individual Joint Control

Selecting the "Arm" control mode instead of the "TV" mode on the mode-select panel (fig. 5) enabled the operator to control the manipulator arm joints. However, since there were five manipulator joints and only two available controller commands (yaw and pitch), the subject had to select the desired joints by using the "Shoulder," "Elbow," and "Wrist" mode switches. Selecting "Shoulder" enabled the subject to command yaw at the manipulator waist and pitch at the shoulder. Selecting "Elbow" enabled yaw at the waist and pitch at the elbow. Selecting "Wrist" enabled yaw and pitch commands to the wrist. The rate of rotation was proportional to the hand-controller deflection. Maximum angular rates were 30 deg/sec at the waist, shoulder, and elbow and 20 deg/sec at the wrist.

Resolved-Rate Control

Rotational rates at manipulator joints can be mathematically transformed and expressed as a combination of linear and angular velocities referenced to a particular coordinate system. The coordinate system is often located at the wrist or in the end effector or tool. In resolved-rate control, linear and angular rates are commanded in an orthogonal axis system, usually in the wrist or end effector (in the probe for this simulation), and the inverse transformation is used to compute corresponding joint rates. Resolved-rate control is useful because it, in effect, decouples the manipulator motion by enabling manual commands to cause orthogonal end-effector motions. Resolved-rate control in several axis systems is the primary manual control mode for the Shuttle Remote Manipulator System, with joint-by-joint control as backup mode. (See ref. 4.)

The simulated resolved-rate control mode was referenced to an axis system fixed in the probe. The subject could command yaw and pitch rates at the wrist and could command linear velocities of ±5 cm/sec (±2 in/sec) in the probe axis system. Resolved-rate control was available when "Arm" and "Wrist" modes were selected. (See fig. 5.) However, in addition to the rotational controller commanding wrist angular rates, the translation command switches used for TV-camera control could be used to command linear velocities of the probe. (Up-down and right-left motions were commanded by switches on the instrument panel, and fore-aft motion was commanded by the speed-brake switch.) For example, if a forward command were made with the speed-brake switch, the computer would automatically compute the joint rotational rates required to cause the probe (and wrist) to move forward along the axis of the probe at 5 cm/sec (2 in/sec).

The resolved-rate equations used in this simulation were derived from differential position changes computed at each 1/32-sec time interval. Similar equations, but of simpler form, are obtained from position derivatives rather than differentials. The derivative form of the resolved-rate equations has been used in subsequent simulations and is presented in the appendix.

TIME DELAYS

Two approaches for real-time remote control of a vehicle in the Earth's orbit are possible. One approach is direct line-of-sight control, either from the ground or from another spacecraft such as the Shuttle or a space station. A single ground station could be in direct contact with a spacecraft for only a fraction of its orbit. If control were from another spacecraft, a similar situation would occur unless the orbital periods of the two were matched. Time delays would not be significant with line-of-sight control, but limiting control to certain time windows would reduce the usefulness of a remote system.

A system of orbiting relay satellites, such as the Tracking and Data Relay Satellite System (TDRSS), is an alternative approach. A TDRSS satellite could relay data between the remote vehicle and the manned control station. When TDRSS is completed, three satellites will provide global coverage. (See ref. 5.) However, use of a relay satellite for real-time control of a remote spacecraft presents several potential problems: First, it has not been done before. Second, the communications bandwidth would limit the rate and/or fidelity of television pictures, probably requiring onboard video preprocessing. Third, data formatting and transmission could introduce time delays. Since round-trip delays using a satellite relay are uncertain, a time delay of up to 2 sec was an independent simulation variable.

Time delays Δt of 0, 0.25, 0.50, 1.0, and 2.0 sec were simulated. Half of the time delay was inserted by passing the control and mode select signals through a holding array prior to the equations of motion in the CDC CYBER 175 computer. The other half of the time delay was inserted by passing signals from the CYBER into a holding array before going to the ADAGE graphics system. In the cockpit, when the operator made a control input, the resulting motion would be seen Δt seconds later. Similarly, a mode change (e.g., from camera 1 to camera 2) would also be delayed Δt seconds.

As noted earlier, the input-confirmation display was never delayed. This was equivalent to superimposing on the (delayed) television picture a graphics display driven directly by control inputs.

PROCEDURE AND ANALYSIS

The simulation was conducted as two separate studies. Five subjects, A to E aged 17 to 25, participated. The first study was a 4 × 2 × 2 factorial design with three replications. Four subjects (A to D) flew each control mode (joint-by-joint and resolved-rate) and two proximity display modes (off or on). The time delay was zero. The order of presentation was joint-by-joint/display off, joint-by-joint/display on, resolved-rate/display off, and resolved-rate/display on. This order was selected because it involved increasing simulation sophistication and enabled the entire simulation to be learned in a logical sequence.

The second study was a 4 × 2 × 5 factorial design with three replications. Four subjects (B to E) flew each control mode with five time delays (0, 0.25, 0.50, 1.0, and 2.0 sec). Three subjects had participated in the first study. The proximity-sensor display was operational for all runs. Two subjects began with the joint-by-joint control mode; the other two subjects began with the resolved-rate control mode. Time delays were presented in a random order.

Subjects were instructed that the objective was to align and insert the probe into each hole on the task board (fig. 3), in a given sequence, starting and ending at the same hole. A different path was followed for each replication, as shown in figure 8, and the paths were presented in random order. Subjects were instructed that although time to complete the task would be recorded, accurate alignment was more important than time. If the probe reached the hole with a tip-displacement error greater than the radius of the hole (1.3 cm (0.5 in.)), the subject would get a visual indication of impact. (See fig. 9.) If an impact occurred, the subject was to withdraw the probe, realign, and make a successful insertion before proceeding to the next hole. Alignment errors at insertion and at impact were recorded.

In addition to recording the time required to complete the task, the number of impacts, and the alignment accuracy, the total number and duration of manipulator control inputs were recorded for each control axis. Inputs were not recorded during control of the simulated TV cameras, but final camera locations were recorded.

An analysis of variance (ref. 6) was performed on the data. Total task time was based on three replications. Angular misalignment and displacement errors for successful insertions were analyzed based on 18 insertions (6 holes × 3 replications).

RESULTS AND DISCUSSION

Effects of Control Mode and Proximity Display

Table I shows the mean alignment error (angular and radial displacement) of the probe tip for 18 insertions (6 holes × 3 replications) for each subject in the first simulation (no time delay). Table II shows the mean, root mean square (rms), and chi-square (χ^2) value of the error over insertions and subjects. The rms errors are presented instead of the standard deviation (σ) because much of the data show strong positive skewness. A chi-square goodness-of-fit test (see ref. 6) rejected the hypothesis that the data came from a normally distributed population at the 0.01 level (table II) for all except radial-displacement errors associated with joint-by-joint control. Figures 10 and 11 show histograms of the alignment errors. The data in tables I and II indicate the following results:

(1) The proximity display had a large effect on angular-alignment accuracy, but no effect on radial-displacement-alignment accuracy.

(2) The control mode had a large effect on both angular and radial-displacement-alignment accuracy.

(3) Differences in subjects had little effect.

When the proximity display was used with resolved-rate control, subjects consistently achieved precise alignment. The display and the resolved-rate control mode were well-matched because the display decoupled or separated the rotational- and translational-alignment errors and the decoupled controls made corrections easy. The subject would rotate the probe until the arms of the cross icon were of equal length, then translate the probe until the center line of the probe (fig. 6) was centered on the hole, and then translate forward for insertion.

Without the proximity display, subjects used the same technique but the rotational alignment was made by using the two orthogonal TV views. The TV views gave less-precise cues so that the rotational-alignment errors were larger. Insertion was still performed by placing the probe center line on the hole and translating forward. This did not require the proximity display, and the data in table I confirm that the proximity display had no effect on displacement errors.

In the joint-by-joint control mode, the proximity display was much less helpful. Despite the precise cues provided for angular-alignment error, the subjects could not effectively decouple the motions because rotation of any joint resulted in both a rotation and a translation of the probe with respect to the task board. Because of this, subjects chose two methods of aligning the probe for insertion by using joint-by-joint control. One method was to minimize alignment errors a short distance in front of the hole, and then to accept the resulting errors on insertion. The other method was to deliberately establish small errors so that they would go to zero on insertion.

These methods were not completely successful, as indicated in table III by the number of impacts. The proximity display had no effect on the number of impacts in the joint-by-joint control mode. With the resolved-rate control mode, there were five impacts without the proximity display but only one impact when using the display.

The time required to complete the task (table IV) shows control-mode effects clearly because the time required to move the probe between holes as well as the alignment time is included. Generally, the time required to complete the task in joint-by-joint control mode was two to three times longer. Table IV also shows that subject B spent two to three times longer than subject A. However, since the subjects were instructed that time was not critical, no operational conclusions should be drawn.

Table V shows the average number and duration of control inputs during a replication. Some subjects often used joint-by-joint control to move the arm close to the task board before beginning the sequence of alignment tasks using resolved-rate control, probably because large rapid movements could be made faster by using joint-by-joint control. The proximity display apparently had no effect on the inputs, but the number of inputs appears directly related to the time required to complete the task. However, the simulated task enabled subjects to use very few inputs in the resolved-rate control mode. Since the task board was assumed planar, after once having aligned the probe with the first hole, the subject had only to translate the probe to subsequent holes. A three-dimensional task board would have required translation and rotation at each hole.

Effect of Control Mode and Time Delay

In the second study, which was a 4 × 2 × 5 factorial design, four subjects performed the alignment task with both control modes, with proximity display on, and with five time delays (~0, 0.25, 0.50, 1.0, and 2.0 sec). Three of the four subjects (B, C, and D) had participated in the first study (no time delays), and their results were used for the zero-time-delay case.

Table VI shows the mean angular- and radial-alignment errors for each subject, and the mean and rms errors over all subjects. The time delays had no effect on the alignment errors. It should be noted that without the proximity display, the angular errors would probably have been greater, as was shown in the first study.

Table VII presents the time required to complete the simulated task. The table shows a large variation with subjects using the joint-by-joint control mode. Some of the variation is due to the control technique used by each subject and the time spent in final alignment. Another source of variation is the time required to repeat an alignment when an impact occurred. Table VIII presents the number of impacts during the test. The number of impacts appears to depend on the subject (and control technique) and control mode, but not on the amount of time delay.

The data in table VII indicate that the time required to complete the task was strongly influenced by both the time delay and the control mode. The time to complete the task, averaged over the subjects, is plotted in figure 12. Considering the variation in the completion times for individual subjects (table VII), the average completion time is remarkably linear for both control modes. The linear relation between task-completion time and time delay is consistent with an earlier study by Ferrell (ref. 7) for a master-slave manipulator task. Ferrell found that the relation between completion time and delay was essentially linear for a given task, the main effect being due to the time spent waiting for feedback. Ferrell postulated that if the operator controlled the remote device by turning motors on and off rather than by using the master-slave control, a similar move-and-wait strategy would be used, and a similar linear relation would occur between completion time and time delay.

This simulation relates directly to Ferrell's prediction. The joint-by-joint control mode was analogous to an on-off control where the rate was selected by the subject. The resolved-rate control mode was a rate-controlled task.

The solid lines in figure 12 are least-squares fits to the experimental data. The completion time using joint-by-joint control T_J is given by

$$T_J = 460 + 399\ \Delta t$$

the completion time using resolved-rate control T_R is given by

$$T_R = 137 + 145\ \Delta t$$

and the dashed line in figure 12 is given by

$$T_R = \frac{1}{3} T_J$$

The good fit of the dashed line to the experimental data in figure 12 indicates that not only were the average completion times directly related to time delay but, with any delay, the completion times for the two control modes also appear to be directly related. The relation between time delay, control mode, and task-completion time found in this study suggests that possible relations might be observed in other studies.

Input Display

The confirmation display (fig. 7) was used in both studies and, therefore, its value cannot be quantified. Subjects commented that the display was not distracting and that it was most useful with the longer time delays for confirming that the computer had received the command and that a result would eventually appear.

An unexpected benefit of the display was shown when a wire behind one of the input switches broke during the simulation. The sudden loss of confirmation of that input suggested an open signal line and resulted in rapid fault isolation.

Location of Simulated Cameras

An advantage of a computer-generated display, such as that used in this simulation, is the ability to position the lookpoint (simulated-camera location) at any desired location. Subjects were encouraged to move the simulated cameras extensively during the familiarization phase. As a result, two camera locations were subjectively identified which were, somewhat surprisingly, satisfactory to all the subjects. Although subjects could reposition the cameras at any time, they were moved in only 7 percent of the data runs. One camera was positioned 87° laterally and 4° vertically with respect to the center of the task board. Camera pan and tilt angles were slightly different (96° and -3°, respectively) in order to include the manipulator arm as well as the task board in the 60° camera field of view. The view from this location (fig. 13(a)) was almost down the side of the task board. It provided horizontal- and vertical-displacement cues, but no lateral-displacement cues. The other camera location was above the task board looking down, 9° laterally and 70° vertically with respect to the center of the task board, and sufficiently far back that the shoulder of the manipulator was visible. (See fig. 13(b).) The corresponding camera pan and tilt angles were 1° and 72°, respectively. This view provided good lateral-displacement cues, but poor vertical and horizontal cues.

Although subjects could move the simulated cameras at any time, in only 11 of the 156 tests was a camera moved from the initial location. In nine tests, the "side" camera was positioned within the range from 79° to 88° laterally and 0° to 6° vertically. In seven tests the "overhead" camera was positioned within the range from 8° to 18° laterally and 68° to 71° vertically.

Thus, throughout the simulation the subjects used essentially orthogonal views from the two cameras to position the manipulator. This is consistent with results of a recent study by Winey (ref. 8) which involved a computer graphic simulation of a seven-degree-of-freedom slave manipulator controlled by an actual master controller having force-reflecting capability. Shadows, multiple views, and proximity indicators were evaluated to determine their effectiveness in giving depth information. In a task of grasping fixed and moving simulated spheres, Winey (ref. 8) found that front and side orthographic projections showed the best performance. Three of the four subjects preferred the orthographic display because they felt it gave the clearest detail. However, reference 8 notes that the best depth indicator would probably be a combination of the front and side views with a shadow.

In this simulation, none of the subjects reported any difficulty in assimilating the data from the three simulated TV scenes (including the probe view) presented on a single monitor, or in manually selecting the desired scene.

POSSIBLE FUTURE STUDIES

As was noted earlier, this simulation used the initial version of a Teleoperator/Robotic System Simulation (TRSS), which will evolve in sophistication to support the technology required for remote space operations. In the course of this simulation, a number of follow-on studies were suggested, some of which are discussed as follows:

(1) Simulation of a three-dimensional task: The simulated two-dimensional task board made the alignment task trivial for a subject using resolved-rate control. A three-dimensional task would be more realistic.

(2) Reduced bandwidth display: For a space task it is likely that the return signal will be bandwidth limited. The bandwidth can be reduced by reducing the television frame rate, reducing the television resolution, limiting the shades of gray, using onboard signal processing (e.g., multiplexing), and/or using onboard image processing (returning only significant features of the scene, such as edges, corners, or motions). Studies (refs. 9 and 10) have examined some of these methods for remote control of underwater manipulators, and some of these results may be applicable to space operations also.

(3) Simultaneous video display: An alternative to selecting a single video display manually from several options would be to present all views simultaneously. This would reduce the manual work load, but it might increase the mental work load as the subject tried to assimilate visual inputs, particularly if the multiple views were presented at lower frame rates.

(4) Six degrees of freedom with end effector: For the simulated alignment task, only five degrees of manipulator freedom were simulated. Generally, a manipulator

will have six or seven degrees of freedom plus an end effector. A sixth degree of freedom, corresponding to rotation about the axis of the probe, and a parallel-jaw end effector are being added to the simulation. This will enable simulation of grasping and turning as well as alignment tasks.

(5) Laboratory comparison: The joints, links, and end effectors of the simulated manipulator represent the actual manipulators in the Langley Intelligent Systems Research Laboratory (ISRL). A study comparing a simulated manipulator task with the same task performed by using actual hardware would validate the simulation and would be a base line for future studies.

(6) Type of visual presentation: In this study, none of the subjects reported any difficulty in assimilating the data from the three simulated TV scenes. In the study reported in reference 8, the front and side orthographic projections were displayed side by side on a single monitor. Other studies have compared single-camera, dual-camera, and stereoscopic display systems and have found that the preferred system depended upon task, camera location, and display bandwidth. By coupling the manned control station in ISRL, which has a stereo-vision system, to the ISRL manipulators through the simulation, it will be possible to compare direct vision, mono and stereo TV, and mono and stereo computer-graphics displays in a manipulator control task.

(7) Sensor models and force/torque control: The manipulator in ISRL has several sensor feedbacks that are not presently modeled in TRSS, including motor currents (or torques) at each joint, three forces and three torques at the manipulator wrist, and two forces and two torques at the jaws of the end effector. These feedbacks make it feasible to command forces and torques and to control the compliance of the end effector or tool. These sensor signals and control modes should be modeled in TRSS in order to simulate general tasks such as touch, grasping, and insertion. The ability to simulate a generic task such as insert-push-turn performed under manual control, or under automatic control with manned supervision, is a goal in the development.

CONCLUDING REMARKS

A simulation has been conducted to examine the effects of two control modes (joint-by-joint and resolved-rate), a visual-proximity-cue display, and time delays (up to 2 sec) on the control of a five-degree-of-freedom manipulator performing a probe-in-hole alignment task. A high-speed computer-graphics system generated the simulated television (TV) scene for three cameras, two of which could be moved in translation and rotation by the subject. However, the subject had to select the scene to be presented on a single TV monitor.

Results showed that all subjects preferred to position the two movable cameras to supply essentially orthogonal views, with one camera looking in from the side of the task and the other looking down from a location above and behind the manipulator. A nominal camera location was identified during familiarization runs and, although subjects could reposition the cameras at any time, they were moved in only 7 percent of the data runs. Subjects had no difficulty selecting and using the single display with multiple simulated cameras.

As expected, subjects preferred the resolved-rate control mode over the joint-by-joint control mode. Not only were alignment errors lower with resolved-rate control, but also less time and fewer inputs were required to accomplish the task, thus indicating a lower subject work load. If a metric for mental and physical work load could be developed, it would be a useful tool for future studies.

The proximity display provided accurate range and angular-alignment information from four assumed, equally spaced, simulated sensors. The proximity display was superimposed on the view from a simulated TV looking along the axis of the probe (the third TV viewing option), and it enabled subjects to differentiate probe-displacement errors from angular errors. Use of the proximity display had no effect on the radial-alignment (displacement) errors, thus suggesting that the displacement-error cues provided by the two orthogonal TV views were as effective as the displacement cues from the proximity display. However, the angular-alignment errors were significantly lower (with either control mode) when the proximity display was used.

The proximity display and the resolved-rate control mode together made the alignment task almost trivial, because the display resolved rotational and translational errors and the control mode enabled them to be controlled separately. The task was made easier by the assumption of a planar task board. Additional studies with a nonplanar task would be desirable.

Time delays were simulated as a transport delay, with half the delay between the control input and the simulated manipulator response and half the delay between the manipulator response and the visual display. The delays forced the subjects to adopt a move-and-wait control strategy for all simulated delays (0.25 sec and longer), but delays had no effect on alignment accuracy.

The major effect of a simulated time delay was to increase the time required to complete the task. The average time required to complete the task increased directly with time delay, with the task time for the joint-by-joint control mode increasing at a greater rate. The relation between the task time for the two control modes was almost constant - about 3.3 times greater for the joint-by-joint control mode. The direct relation between time delay, control mode, and task-completion time should be tested in subsequent studies.

A useful feature of the simulation was an unobtrusive indicator which was displayed during manual-control inputs. The indicator was superimposed on the visual display and confirmed the type (translation or rotation) and direction of the input. It was most useful with longer time delays because it verified that the computer had received the input, thereby assuring eventual response.

Langley Research Center
National Aeronautics and Space Administration
Hampton, VA 23665
July 25, 1983

APPENDIX

RESOLVED-RATE EQUATIONS

In resolved-rate control, the operator specifies the rate of end-effector motion (translational and rotational) and a control algorithm transforms these commands into rate commands for the individual joints. The resultant end-effector motion is the sum of all the contributions made by the joints. By expressing end-effector velocity as the sum of joint contributions, a system of equations is obtained that relates end-effector rates to joint rates. The system of equations is linear and can be solved by matrix methods.

The simulated manipulator had five degrees of freedom; therefore, five end-effector motions (three translations and two rotations) could be commanded. Thus,

$$\left\{\begin{matrix} \dot{X} \\ \dot{Y} \\ \dot{Z} \\ \dot{\theta} \\ \dot{\phi} \end{matrix}\right\}_{\substack{\text{end} \\ \text{effector}}} = |J| \left\{\begin{matrix} \dot{\phi}_1 \\ \dot{\theta}_1 \\ \dot{\theta}_2 \\ \dot{\theta}_3 \\ \dot{\phi}_3 \end{matrix}\right\} \tag{A1}$$

where $\dot{\phi}_1$ is the angular rate at the manipulator waist; $\dot{\theta}_1$, $\dot{\theta}_2$, and $\dot{\theta}_3$ are angular (pitch) rates at the shoulder, elbow, and wrist, respectively; and $\dot{\phi}_3$ is the yaw rate at the wrist. (See fig. 1.)

Inverting the Jacobian matrix [J] would give an exact solution for the resolved rates, but performing a 5 × 5 matrix inversion 32 times per second for the real-time simulation was undesirable. A number of methods have been proposed for speeding up the solution of the matrix-inversion problem. One approach is to separate the translational and rotational motion, resulting in two smaller matrices which can be easily inverted. This approach is discussed in reference 11 and was used in the simulation. It was assumed that only the first three joints affected the linear motion; that is, resolved-rate translational commands were referenced to the wrist. In addition,

θ_1, θ_2, and θ_3 were sequential rotations so that the shoulder, elbow, and wrist, respectively, were coplanar. Thus,

$$\begin{Bmatrix} \dot{X} \\ \dot{Y} \\ \dot{Z} \\ \dot{\theta} \\ \dot{\phi} \end{Bmatrix}_{\substack{\text{end} \\ \text{effector}}} = \left|\begin{array}{cccc:c} & & & 0 & 0 \\ & J_3 & & 0 & 0 \\ & & & 0 & 0 \\ \hdashline 0 & 1 & 1 & 1 & 0 \\ 1 & 0 & 0 & 0 & 1 \end{array}\right| \begin{Bmatrix} \dot{\phi}_1 \\ \dot{\theta}_1 \\ \dot{\theta}_2 \\ \dot{\theta}_3 \\ \dot{\phi}_3 \end{Bmatrix} \tag{A2}$$

$$\dot{\theta} = \dot{\theta}_1 + \dot{\theta}_2 + \dot{\theta}_3 \tag{A3}$$

$$\dot{\phi} = \dot{\phi}_1 + \dot{\phi}_3 \tag{A4}$$

Then,

$$\dot{\theta}_3 = \dot{\theta}_C - (\dot{\theta}_1 + \dot{\theta}_2) \tag{A5}$$

$$\dot{\phi}_3 = \dot{\phi}_C - \dot{\phi}_1 \tag{A6}$$

where $\dot{\theta}_C$ and $\dot{\phi}_C$ are end-effector angular-rate commands from the rotational hand controller in the cockpit.

The terms of the J_3 matrix were referenced to an X,Y,Z axis system, illustrated in figure 14, centered at the manipulator shoulder, with the Z-axis aligned with the ϕ_1-axis of rotation and rotating about Z so that the X-Z plane contained the upper and lower arms and wrist. The position of the wrist was

$$X = L_1 \cos \theta_1 + L_2 \cos(\theta_1 + \theta_2) \tag{A7}$$

$$Y = 0 \tag{A8}$$

$$Z = -L_1 \sin\theta_1 - L_2 \sin(\theta_1 + \theta_2) \tag{A9}$$

The velocity of the wrist, then, is

$$\dot{X} = -L_1 \sin\theta_1 \dot{\theta}_1 - L_2 \sin(\theta_1 + \theta_2)(\dot{\theta}_1 + \dot{\theta}_2) \tag{A10}$$

$$\dot{Y} = X\dot{\psi}_1 \tag{A11}$$

$$\dot{Z} = -L_1 \cos\theta_1 \dot{\theta}_1 - L_2 \cos(\theta_1 + \theta_2)(\dot{\theta}_1 + \dot{\theta}_2) \tag{A12}$$

and

$$\dot{\theta}_1 = \frac{\dot{X}\cos(\theta_1 + \theta_2) - \dot{Z}\sin(\theta_1 + \theta_2)}{L_1 \sin\theta_2} \tag{A13}$$

$$(\dot{\theta}_1 + \dot{\theta}_2) = \frac{-\dot{X}\cos\theta_1 + \dot{Z}\sin\theta_1}{L_2 \sin\theta_2} \tag{A14}$$

$$\dot{\theta}_2 = (\dot{\theta}_1 + \dot{\theta}_2) - \dot{\theta}_1 \tag{A15}$$

$$\dot{\psi}_1 = \frac{\dot{Y}}{X} = \frac{\dot{Y}}{L_1 \cos\theta_1 + L_2 \cos(\theta_1 + \theta_2)} \tag{A16}$$

APPENDIX

The resolved-rate translation commands X_C, Y_C, Z_C from the cockpit were transformed to the X,Y,Z axis system by

$$\begin{Bmatrix} \dot{X} \\ \dot{Y} \\ \dot{Z} \end{Bmatrix} = K|T| \begin{Bmatrix} \dot{X}_C \\ \dot{Y}_C \\ \dot{Z}_C \end{Bmatrix} \tag{A17}$$

where K is an empirical multiplier,

$$|T| = \begin{vmatrix} \cos \phi_3 \cos \alpha & -\sin \phi_3 \cos \alpha & \sin \alpha \\ \sin \phi_3 & \cos \phi_3 & 0 \\ -\cos \phi_3 \sin \alpha & \sin \alpha \sin \phi_3 & \cos \alpha \end{vmatrix} \tag{A18}$$

and

$$\alpha = \theta_1 + \theta_2 + \theta_3 \tag{A19}$$

When $\theta_2 = 0$, equations (A13), (A14), and the J_3 matrix (eq. (A2)) are singular. A matrix inversion would still be possible by using a pseudoinverse matrix solution, but in the simulation the singularity was avoided by limiting θ_2 by using the empirical multiplier K in equation (A17) where

$$K = 1$$

when $|\theta_2| \geqslant 25°$ or $\theta_2 \dot{\theta}_2 \geqslant 0$ and

$$K = \frac{|\theta_2| - 5°}{20°} \tag{A20}$$

when $|\theta_2| < 25°$ and $\theta_2 \dot{\theta}_2 < 0$.

The effect of this limit was to reduce slightly (by 0.2 percent) the maximum extension of the arm and to slow the motion of the arm as it neared maximum extension. This was not a problem for the subjects since all of the simulated task board was within the reach envelope.

REFERENCES

1. Britton, W. R.: Proto-Flight Manipulator Arm (P-FMA). Rept. MCR-77-201 (Contract NAS8-31487), Martin Marietta Corp., Apr. 1977. (Available as NASA CR-150277.)

2. Johnston, A. R.: Proximity Sensor Technology for Manipulator End Effectors. Mech. & Mach. Theory, vol. 12, no. 1, 1977, pp. 95-109.

3. Bejczy, A. K.; Brown, J. W.; and Lewis, J. L.: Evaluation of Proximity Sensor Aided Grasp Control for Shuttle RMS. Fifteenth Annual Conference on Manual Control, Frank L. George, ed., AFFDL-TR-79-3134, U.S. Air Force, Nov. 1979, pp. 404-429. (Available from DTIC as AD A080 563.)

4. McCullough, J. R.; Sharpe, A.; and Doetsch, K. H.: The Role of the Real-Time Simulation Facility, SIMFAC, in the Design, Development and Performance Verification of the Shuttle Remote Manipulator System (SRMS) With Man-in-the-Loop. 11th Space Simulation Conference, NASA CP-2150, 1980, pp. 94-112.

5. Klimek, D.: Tracking and Data Relay Satellite System Performance. 1980 International Telemetering Conference, Instrum. Soc. America, 1980, pp. 247-260.

6. Snedecor, George W.; and Cochran, William G.: Statistical Methods, Sixth ed. Iowa State Univ. Press, c.1967.

7. Ferrell, William R.: Remote Manipulation With Transmission Delay. IEEE Trans. Hum. Factors Electron., vol. 6, Sept. 1965, pp. 24-32.

8. Winey, Calvin McCoy, III: Computer Simulated Visual and Tactile Feedback as an Aid to Manipulator and Vehicle Control. Contract N00014-77-C-0256, Dept. Mech. Eng., Massachusetts Inst. of Technol., May 1981. (Available from DTIC as AD A116 787.)

9. Cole, R. E.; and Kishimoto, B. H.: Remote Operator Performance Using Bandwidth Limited TV Displays: A Review and Proposal. NOSC TD 379, U.S. Navy, Aug. 1980. (Available from DTIC as AD A100 438.)

10. Doelling, Norman: Progress in Underwater Telemanipulator Research, Rev. ed. Rept. No. MITSG-81-4 (NOAA-81102109), Massachusetts Inst. of Technol., July 1, 1981. (Available from NTIS as PB82 148 651.)

11. Lowrie, J. W.; Fermelia, A. J.; Haley, D. C.; Gremban, K. D.; Van Baalen, J.; and Walsh, R. W.: Evaluation of Automated Decisionmaking Methodologies and Development of an Integrated Robotic System Simulation - Appendixes B, C, D, E. NASA CR-165977, 1982.

TABLE I.- ALIGNMENT ERRORS WITHOUT TIME DELAYS

(a) Angular error by subject

Subject	Angular error, deg, for proximity display -			
	Off	On	Off	On
	Joint-by-joint control mode		Resolved-rate control mode	
A	3.9	2.5	1.6	0.4
B	5.5	1.5	1.3	.4
C	4.1	4.0	1.9	.1
D	5.0	.9	2.1	.6
Mean	4.6	2.2	1.7	0.4
rms	6.0	4.3	1.9	0.5

(b) Radial-displacement error by subject

Subject	Radial-displacement error, cm, for proximity display -			
	Off	On	Off	On
	Joint-by-joint control mode		Resolved-rate control mode	
A	0.61	0.66	0.29	0.29
B	.79	.56	.41	.20
C	.50	.53	.24	.35
D	.62	.74	.28	.27
Mean	0.63	0.62	0.30	0.28
rms	0.72	0.72	0.37	0.40

TABLE II.- ALIGNMENT ERRORS WITHOUT TIME DELAYS

(a) Angular error for all subjects

Statistical values	Angular error, deg, for proximity display -			
	Off	On	Off	On
	Joint-by-joint control mode		Resolved-rate control mode	
Mean	4.6	2.2	1.7	0.4
rms	6.0	4.3	1.9	0.5
χ^2 value	37.7	123.2	25.1	50.5
$\chi^2_{0.01}$	16.8	15.1	15.1	13.3
Significant at 0.01	Yes	Yes	Yes	Yes
σ	3.9	3.8	0.7	0.3

(b) Radial-displacement error for all subjects

Statistical values	Radial-displacement error, cm, for proximity display -			
	Off	On	Off	On
	Joint-by-joint control mode		Resolved-rate control mode	
Mean	0.63	0.62	0.30	0.28
rms	0.72	0.72	0.37	0.40
χ^2 value	11.4	15.7	23.4	76.6
$\chi^2_{0.01}$	18.5	16.8	16.8	15.1
Significant at 0.01	No	No	Yes	Yes
σ	0.35	0.36	0.21	0.29

TABLE III.- NUMBER OF IMPACTS

Subject	Number of impacts with proximity display -			
	Off	On	Off	On
	Joint-by-joint control mode		Resolved-rate control mode	
A	2	0	1	0
B	2	4	0	0
C	3	2	3	0
D	2	3	1	1
Total	9	9	5	1

TABLE IV.- AVERAGE TASK TIME FOR THREE REPLICATIONS

Subject	Average task time, sec, for proximity display -			
	Off	On	Off	On
	Joint-by-joint control mode		Resolved-rate control mode	
A	300	226	99	116
B	602	629	296	201
C	319	388	213	125
D	423	437	129	113
Mean	411	420	184	139

TABLE V.- AVERAGE NUMBER AND DURATION OF CONTROL INPUTS FOR A SINGLE REPLICATION

[One replication is equivalent to six alignments]

Control applied	Average number and duration of control inputs with proximity display -							
	Off		On		Off		On	
	Number	Duration, sec	Number	Duration, sec	Number	Duration, sec	Number	Duration, sec
	Joint-by-joint control mode				Resolved-rate control mode			
Waist (yaw)	60.0	33.0	48.5	31.0	1.4	0.2	0.8	0.2
Shoulder (pitch)	64.7	34.3	52.2	30.5	0.5	0.2	0.7	0.3
Elbow (pitch)	110.3	70.8	101.3	63.9	2.2	0.9	0.9	0.7
Wrist (yaw)	27.2	29.3	30.6	27.2	6.5	3.6	9.3	2.9
Wrist (pitch)	25.8	19.5	40.8	28.0	12.8	5.2	16.4	5.3
Fore and aft velocity					20.1	14.6	18.3	15.6
Lateral velocity					33.3	26.1	28.8	25.5
Vertical velocity					27.5	26.6	33.4	26.2
Total	288.0	186.9	273.4	180.6	104.3	77.4	108.6	76.7

TABLE VI.-ALIGNMENT ERRORS WITH TIME DELAYS

(a) Angular error by subject

Subject	Angular error, deg, for time delay of -				
	0 sec	0.25 sec	0.50 sec	1.0 sec	2.0 sec
Joint-by-joint control mode					
B	1.57	1.29	1.40	2.13	1.69
C	3.96	2.27	2.30	1.91	.56
D	.88	1.34	1.33	1.69	1.88
E	1.62	1.87	1.98	1.35	1.69
Mean	2.01	1.69	1.75	1.77	1.46
rms	4.18	2.10	2.09	2.19	1.97
Resolved-rate control mode					
B	0.48	0.48	0.54	0.38	0.29
C	.15	.20	.39	.55	.31
D	.55	.21	.09	.09	.12
E	.04	.04	.11	.06	.18
Mean	0.31	0.23	0.28	0.27	0.22
rms	0.40	0.32	0.41	0.46	0.34

(b) Radial-displacement error by subject

Subject	Radial-displacement error, cm, for time delay of -				
	0 sec	0.25 sec	0.50 sec	1.0 sec	2.0 sec
Joint-by-joint control mode					
B	0.56	0.64	0.78	0.99	0.84
C	.53	.46	.54	.71	.80
D	.74	.80	.85	.75	.65
E	.36	.43	.46	.41	.46
Mean	0.55	0.59	0.66	0.72	0.69
rms	0.65	0.68	0.76	0.81	0.77
Resolved-rate control mode					
B	0.20	0.17	0.18	0.24	0.24
C	.23	.19	.27	.36	.31
D	.27	.25	.24	.21	.17
E	.14	.19	.20	.15	.20
Mean	0.21	0.20	0.22	0.24	0.23
rms	0.24	0.22	0.25	0.30	0.29

TABLE VII.- AVERAGE TASK TIME WITH TIME DELAYS

Subject	Average task time with time delay of -				
	0 sec	0.25 sec	0.50 sec	1.0 sec	2.0 sec
Joint-by-joint control mode					
B	629	630	633	895	1147
C	388	484	552	977	1842
D	437	809	943	930	1139
E	419	356	400	672	912
Mean	468	570	632	869	1260
Resolved-rate control mode					
B	201	259	194	263	380
C	125	211	201	300	582
D	113	179	184	221	329
E	130	137	190	242	468
Mean	142	196	192	257	440

TABLE VIII.- NUMBER OF IMPACTS WITH TIME DELAYS

Subject	Number of impacts with time delay of -				
	0 sec	0.25 sec	0.50 sec	1.0 sec	2.0 sec
Joint-by-joint control mode					
B	4	6	1	2	3
C	2	2	1	0	4
D	3	1	3	1	0
E	0	0	0	0	1
Total ...	9	9	5	3	8
Resolved-rate control mode					
B	0	0	0	0	0
C	0	↓	↓	↓	2
D	1	↓	↓	↓	0
E	0	↓	↓	↓	0
Total ...	1	0	0	0	2

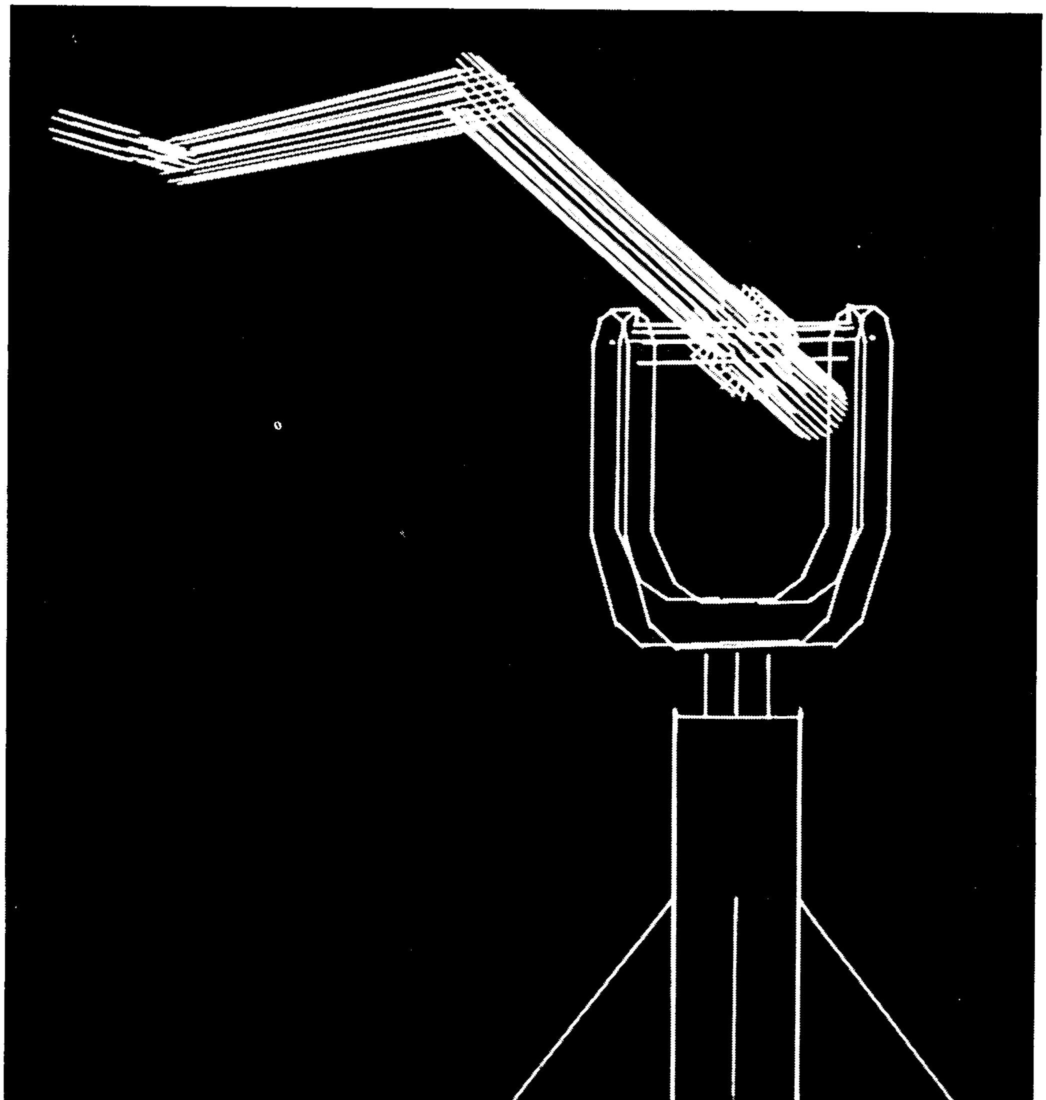

L-82-839

Figure 1.- Computer-generated image of simulated manipulator.

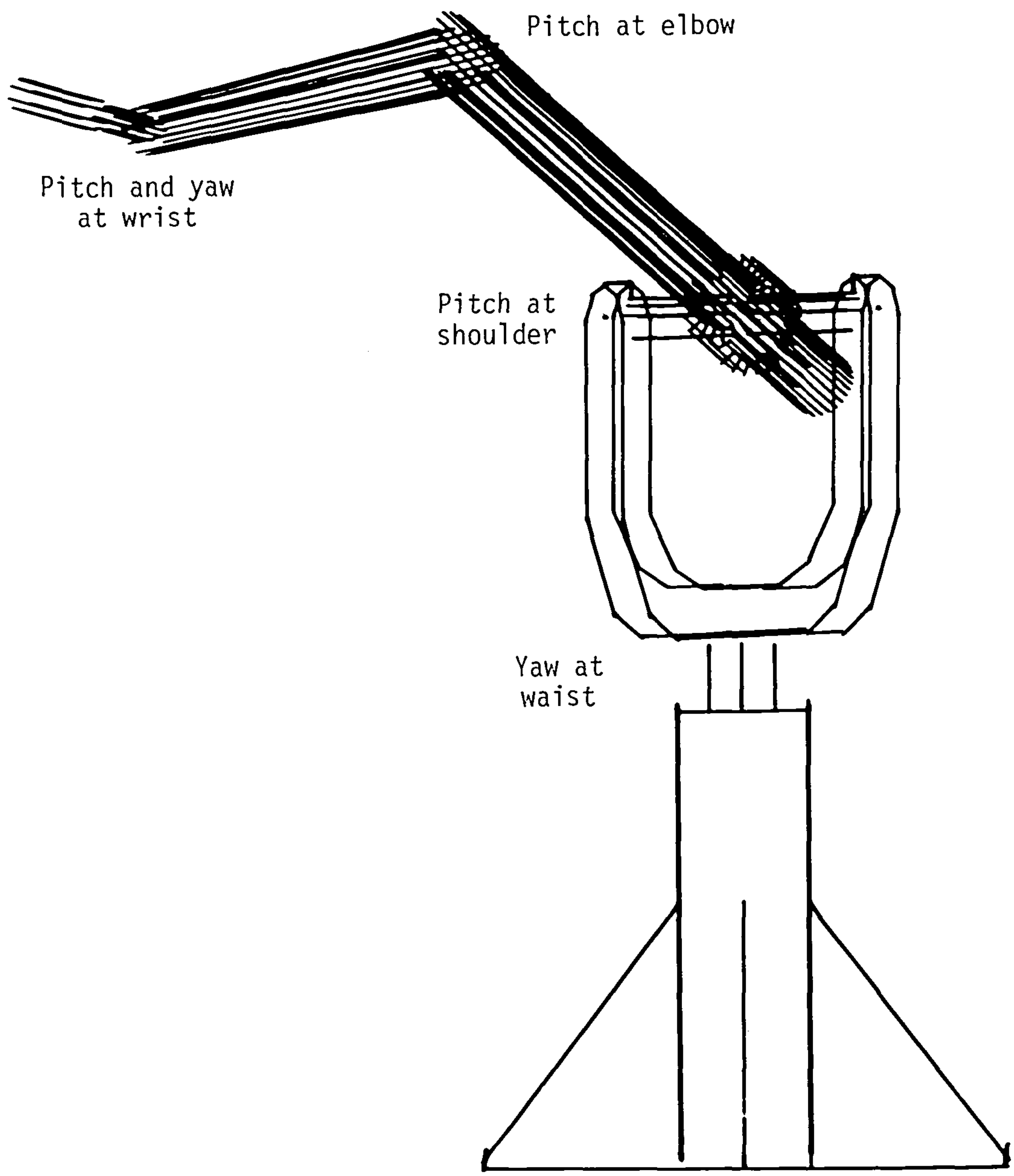

Figure 2.- Configuration of simulated manipulator.

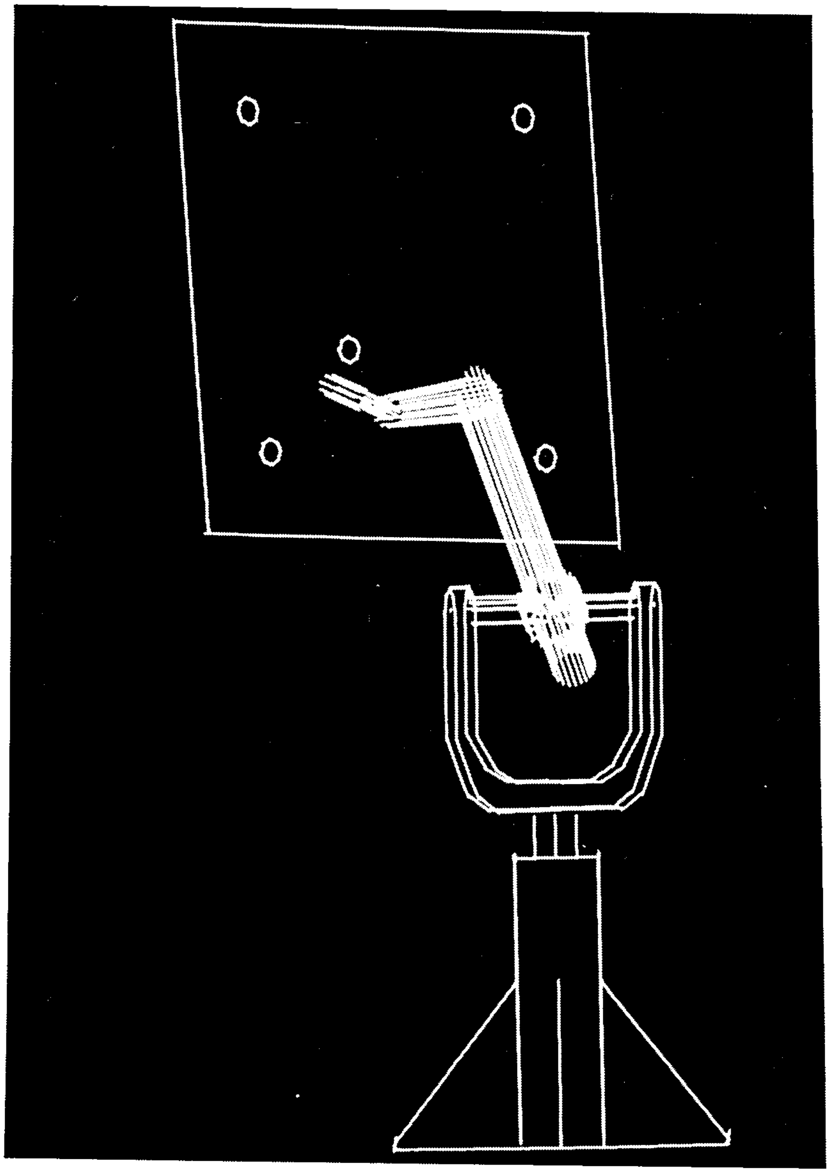

L-82-841

Figure 3.- Simulated task board.

L-82-4117

Figure 4.- Simulator cockpit.

Camera 1	Arm		Shoulder
Camera 2	TV		Elbow
Probe TV	Proximity display		Wrist
Reset TV			

Figure 5.- Mode-select panel located on left side of instrument panel.

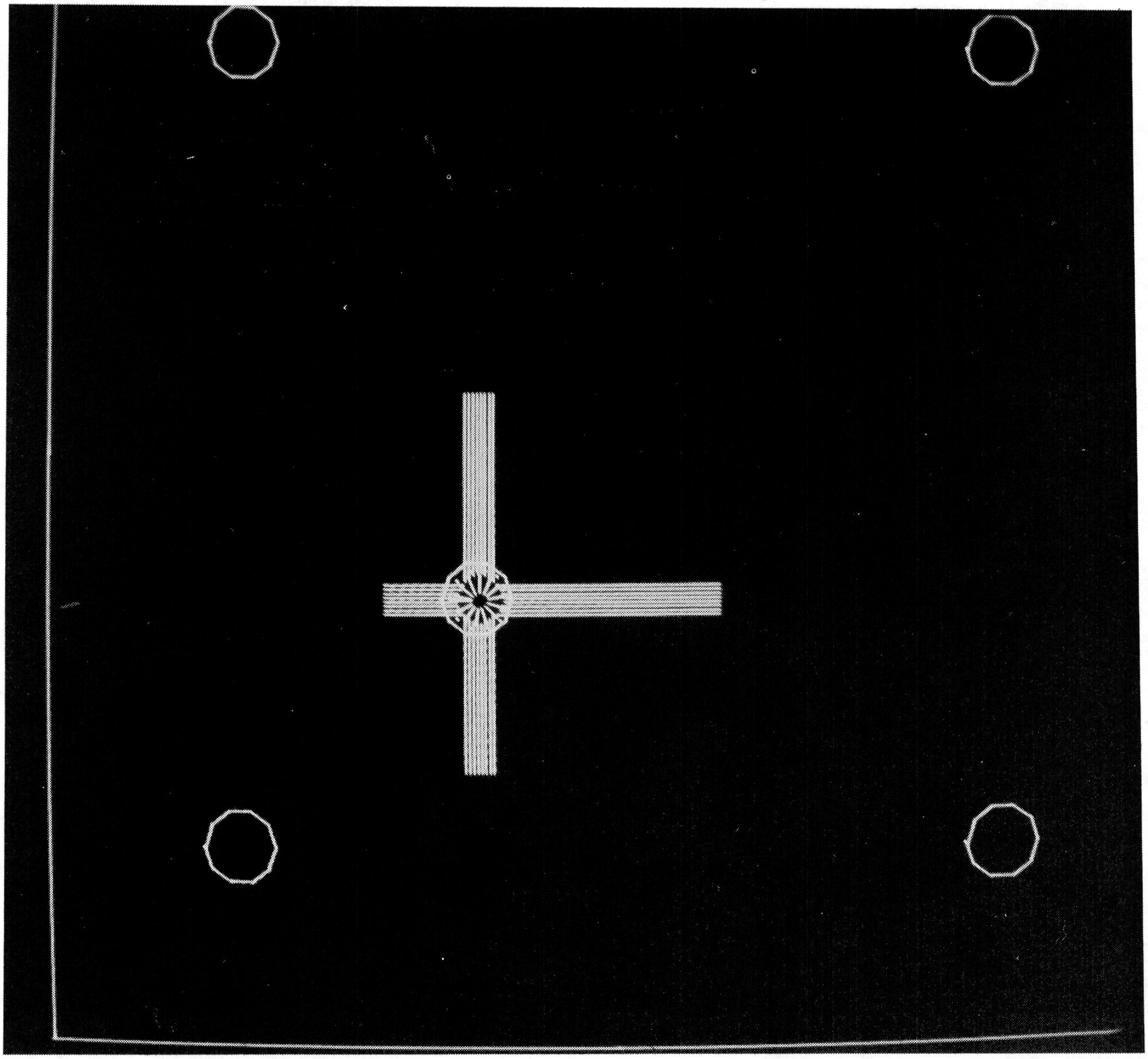

L-82-11,111

Figure 6.- Simulated proximity display showing lateral (yaw) angular misalignment.

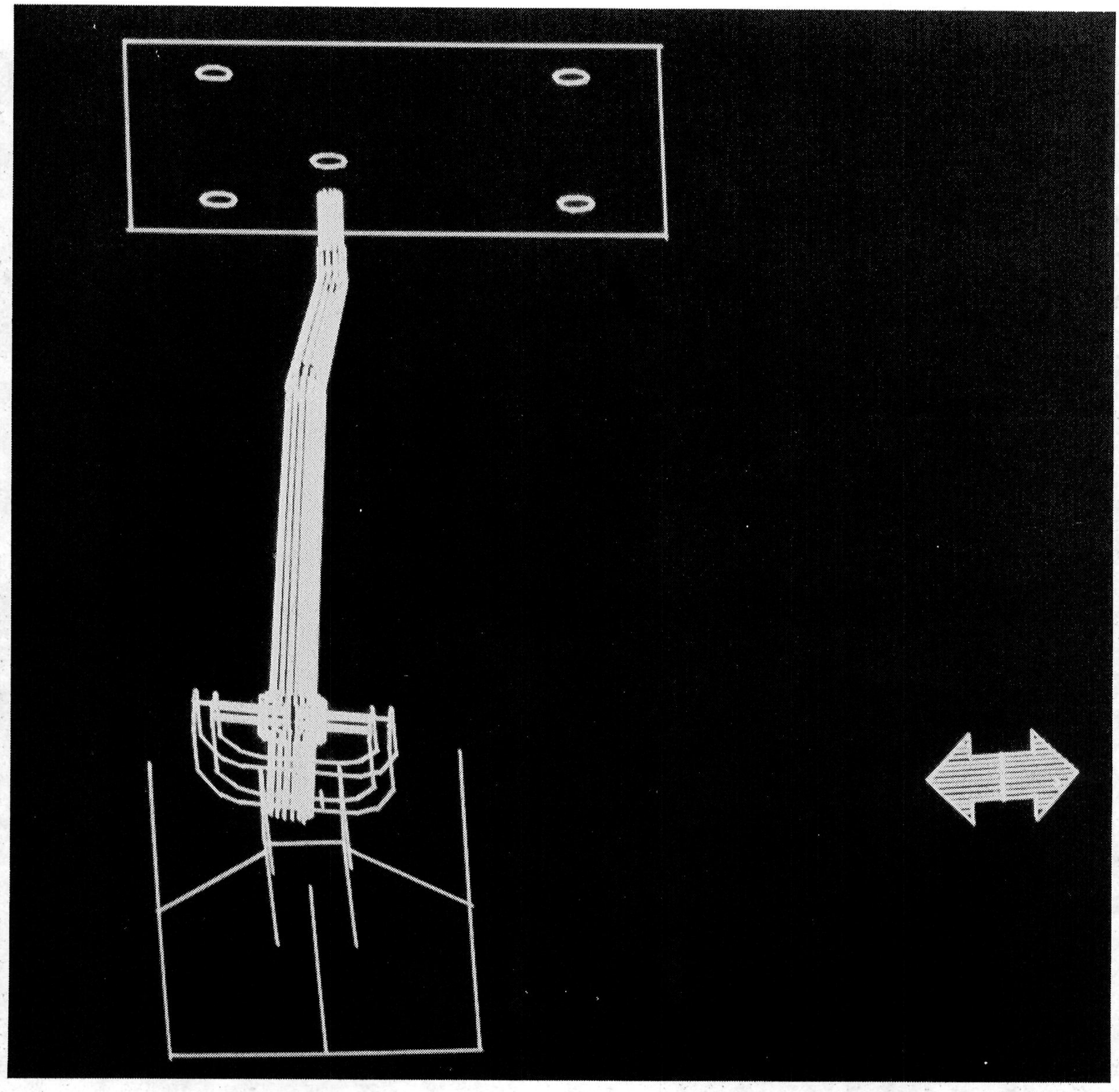

L-82-11,108

(a) Lateral-translation indicator.

Figure 7.- Simulated display showing control confirmation in lower right corner.

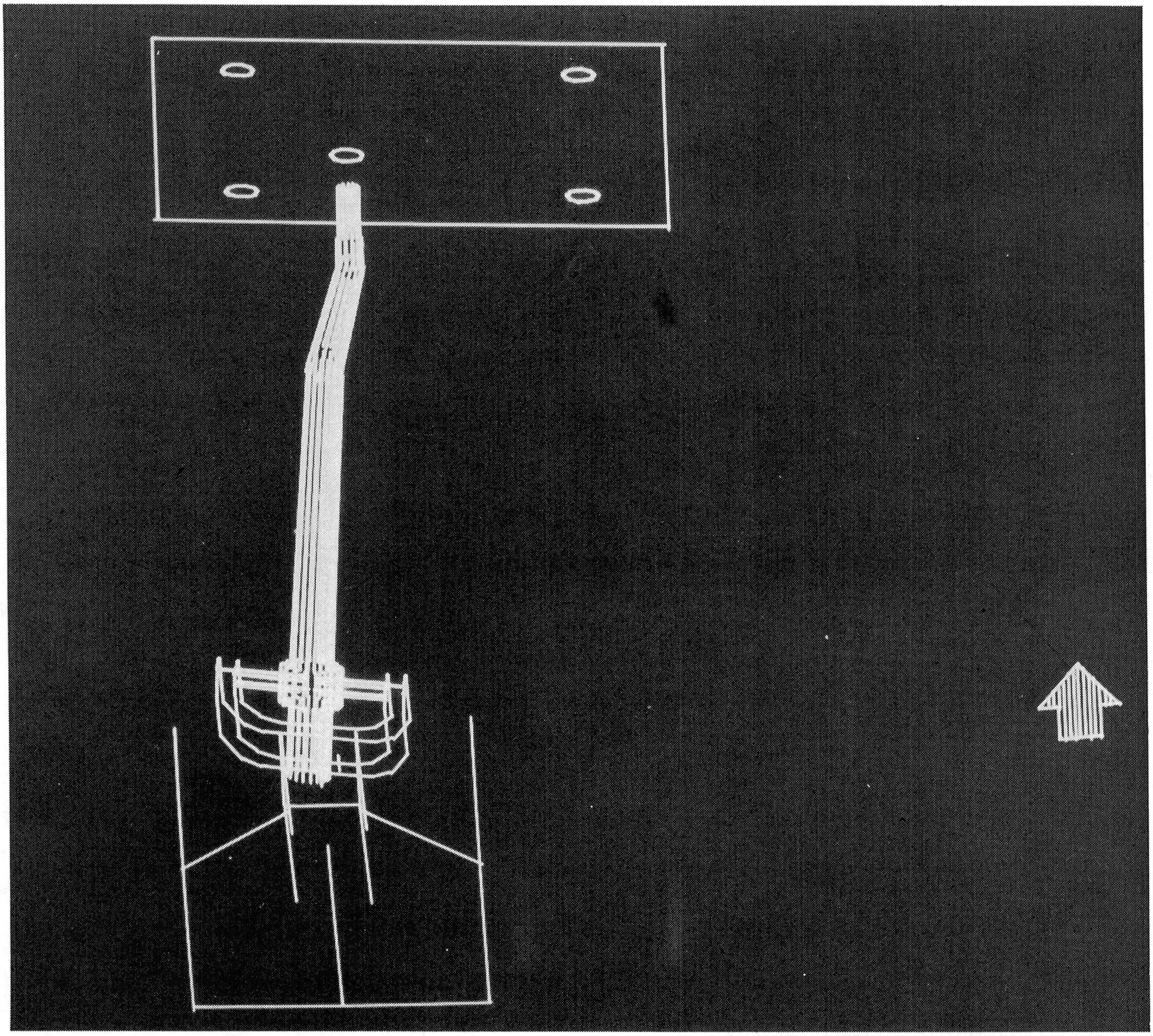

L-82-11,110

(b) Pitch-up indicator.

Figure 7.- Concluded.

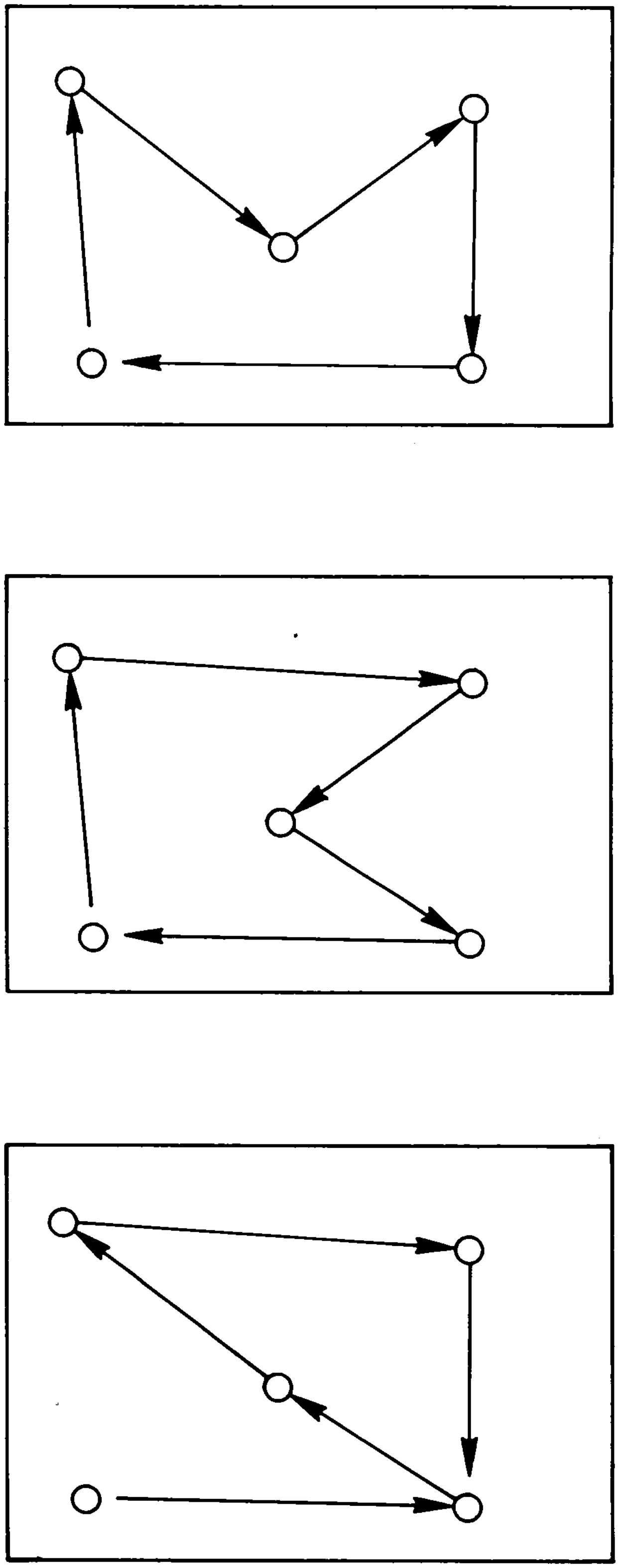

Figure 8.- Path (sequence of holes) followed
in tests.

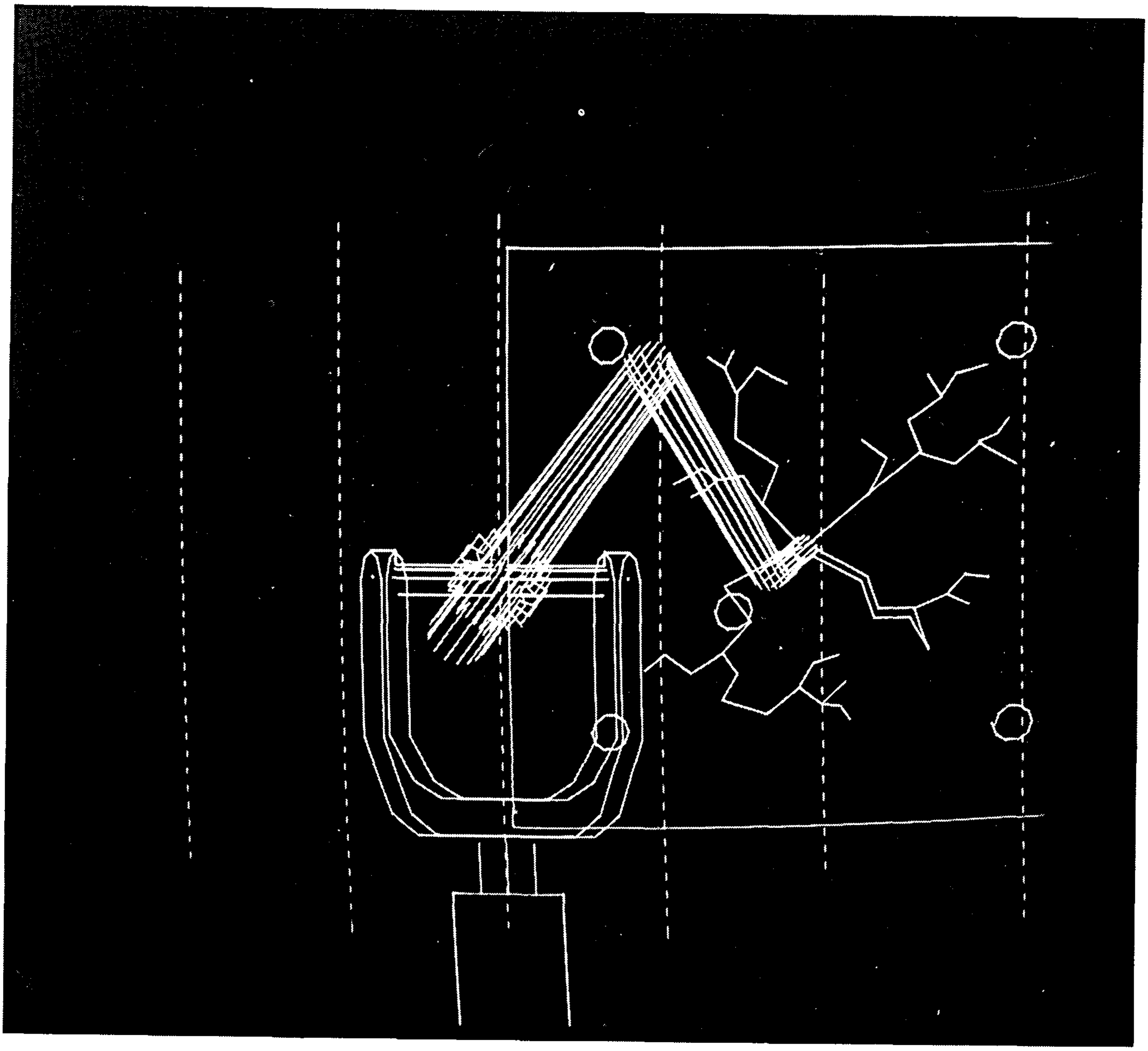

Figure 9.- Impact display.

L-82-4109

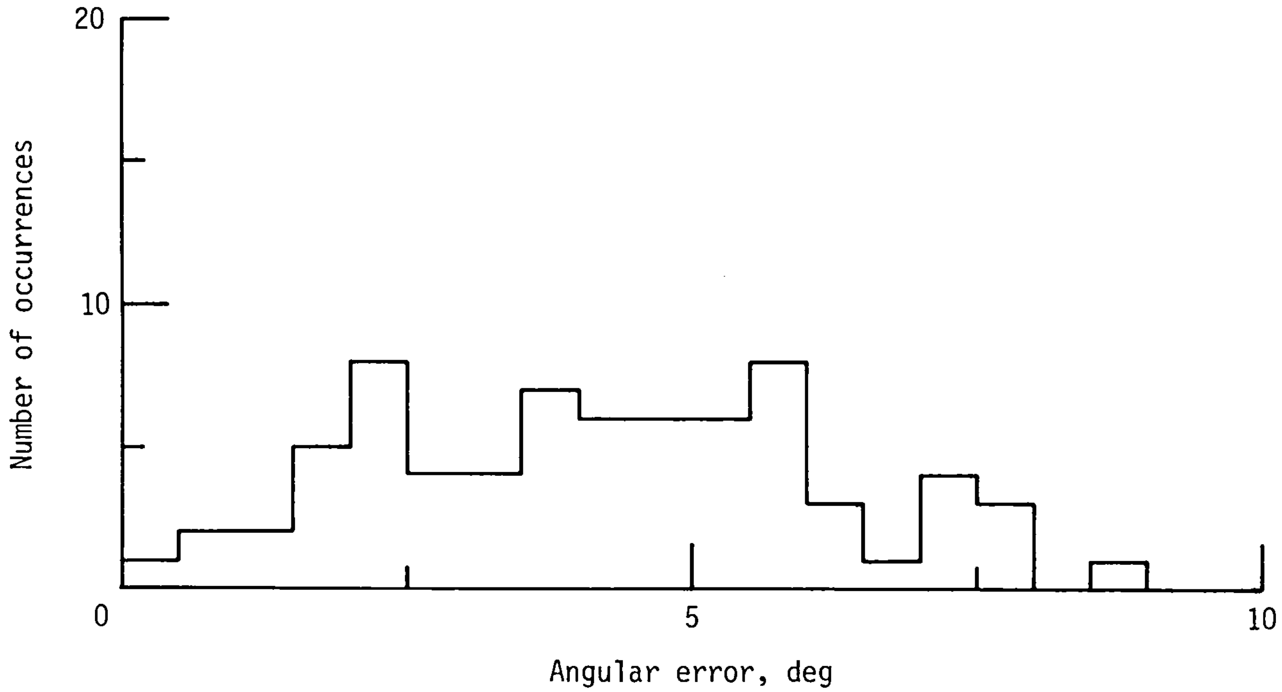

(a) Joint-by-joint control. Proximity display off.

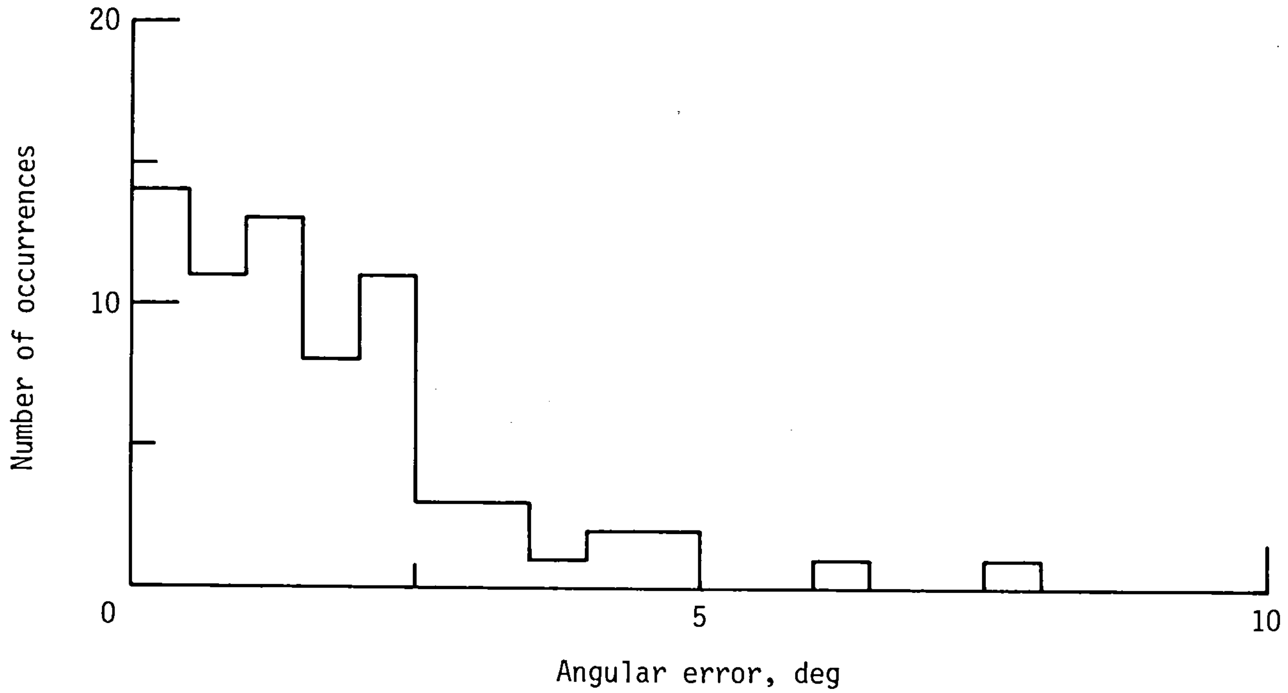

(b) Joint-by-joint control. Proximity display on.

Figure 10.- Histogram of angular-alignment error.

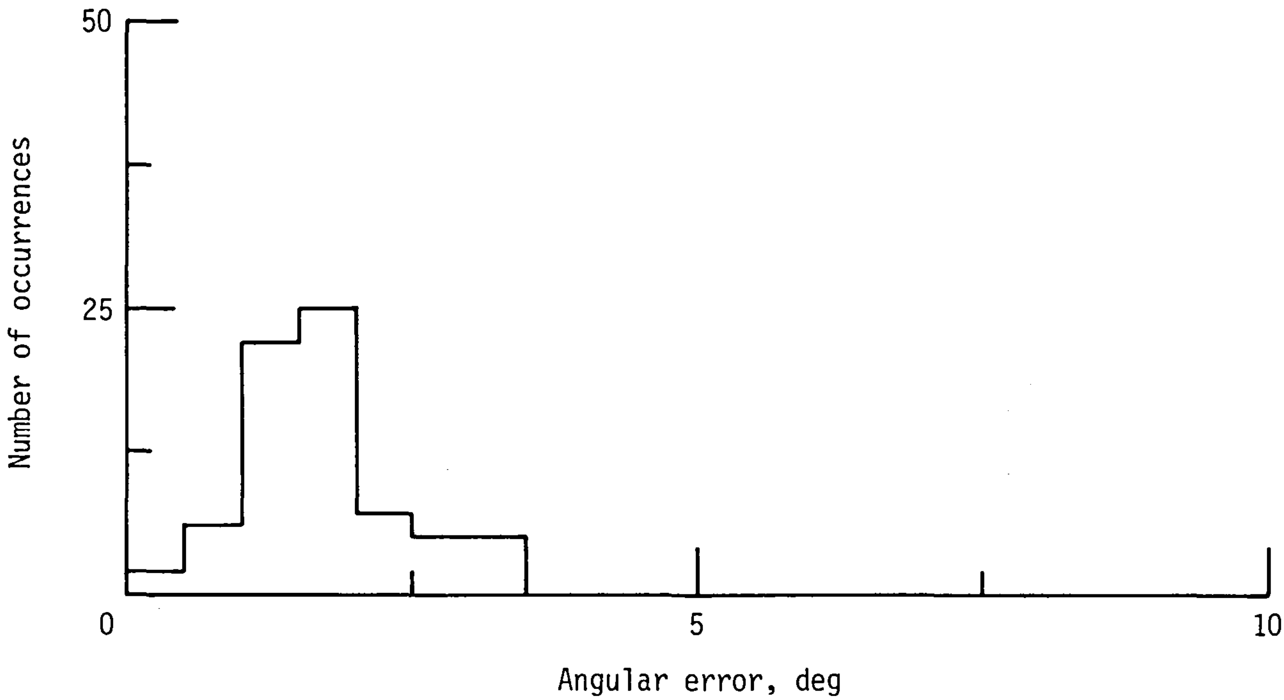

(c) Resolved-rate control. Proximity display off.

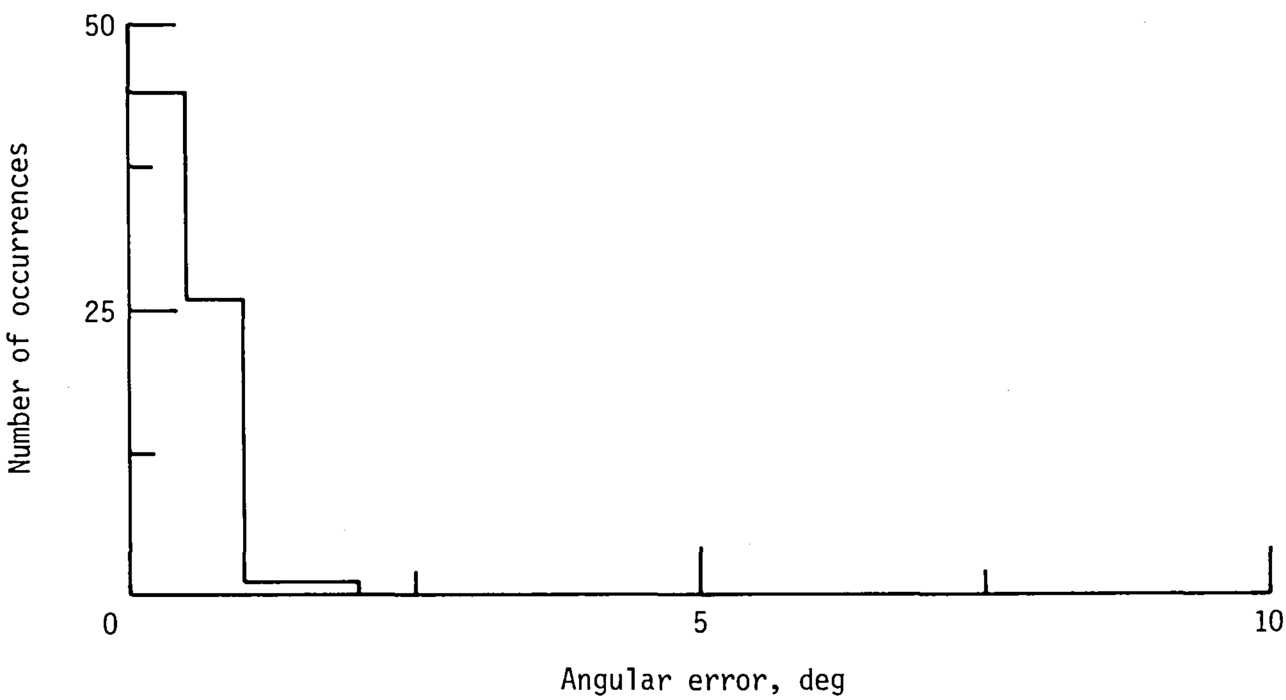

(d) Resolved-rate control. Proximity display on.

Figure 10.- Concluded.

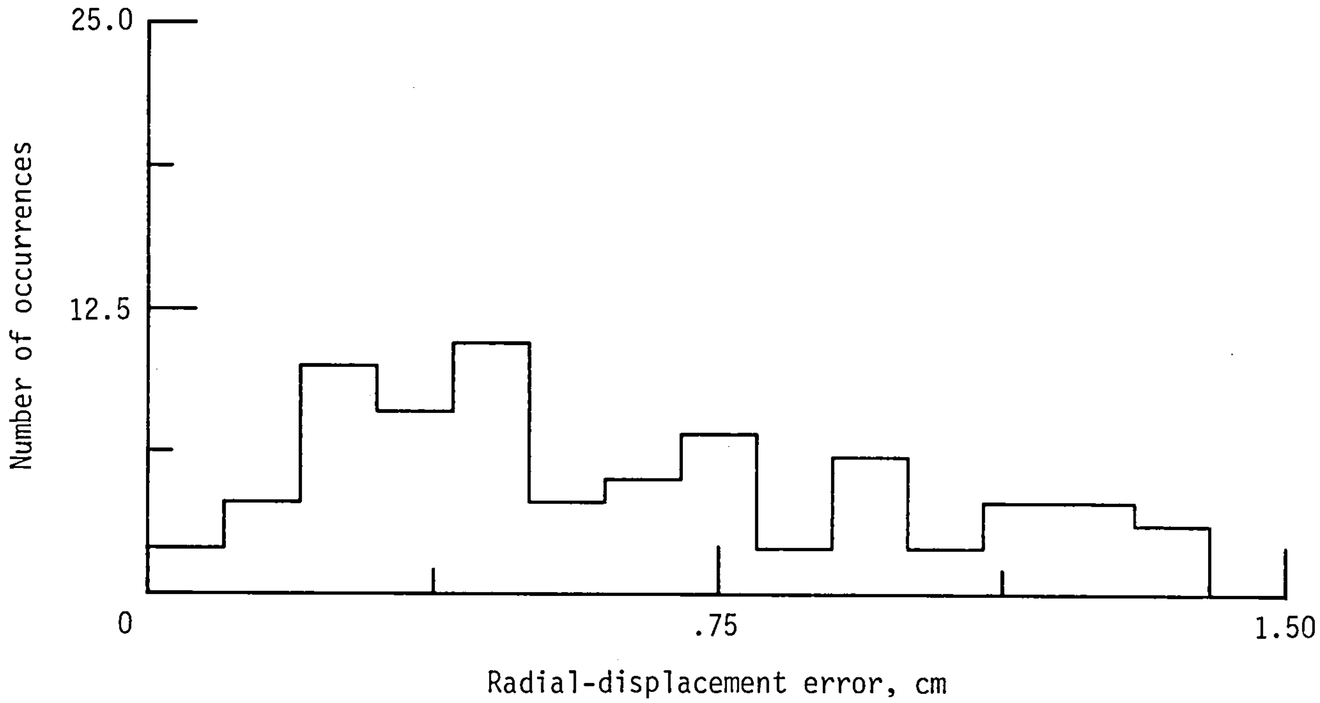

(a) Joint-by-joint control. Proximity display on.

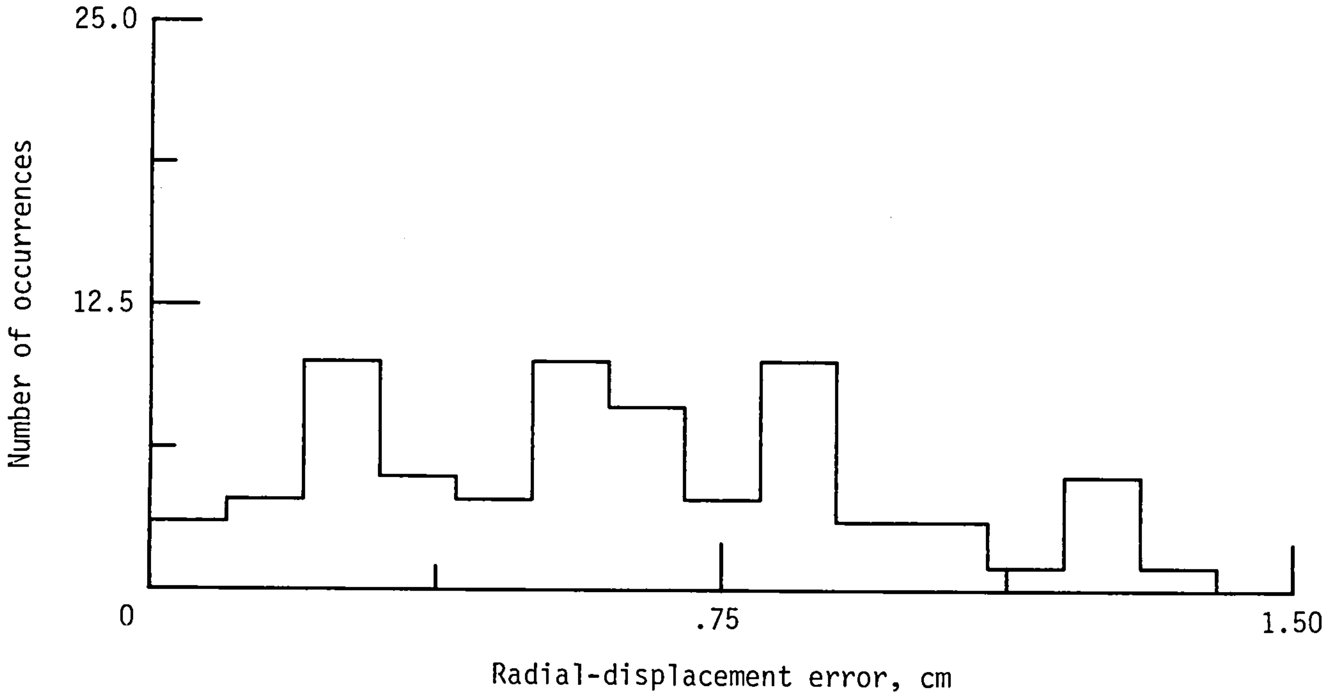

(b) Joint-by-joint control. Proximity display off.

Figure 11.- Histogram of radial-alignment error.

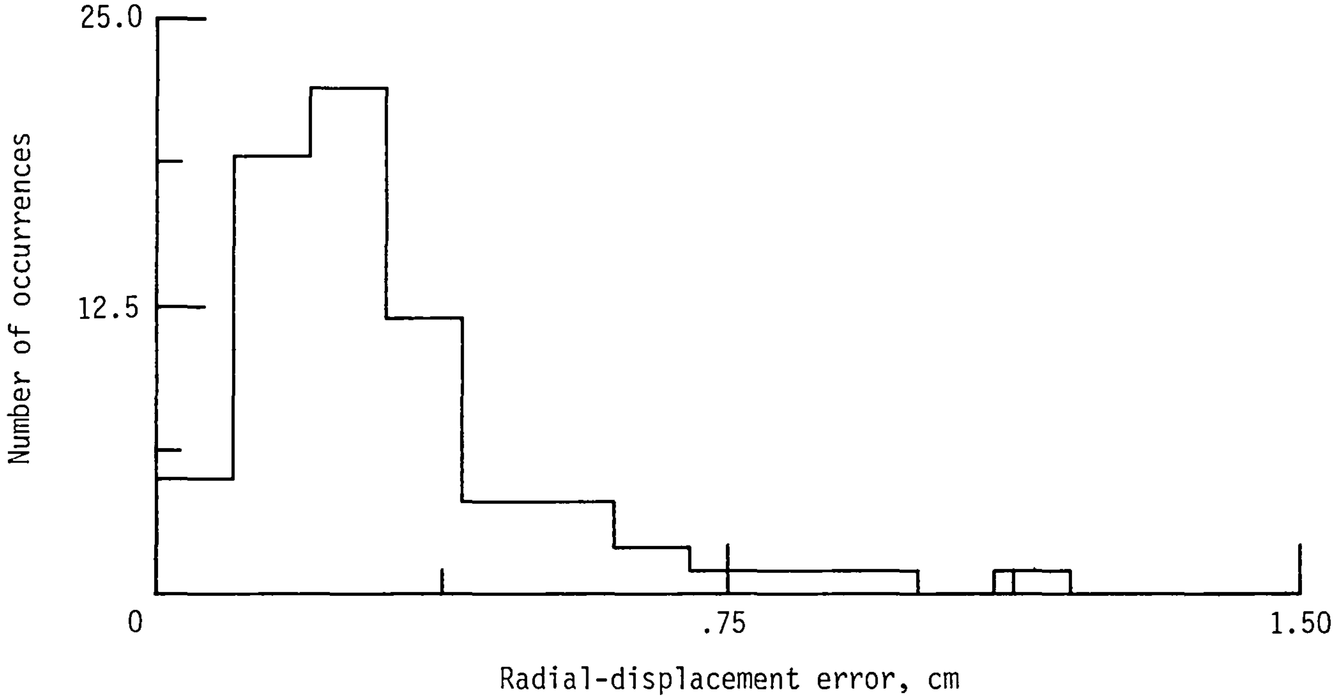

(c) Resolved-rate control. Proximity display off.

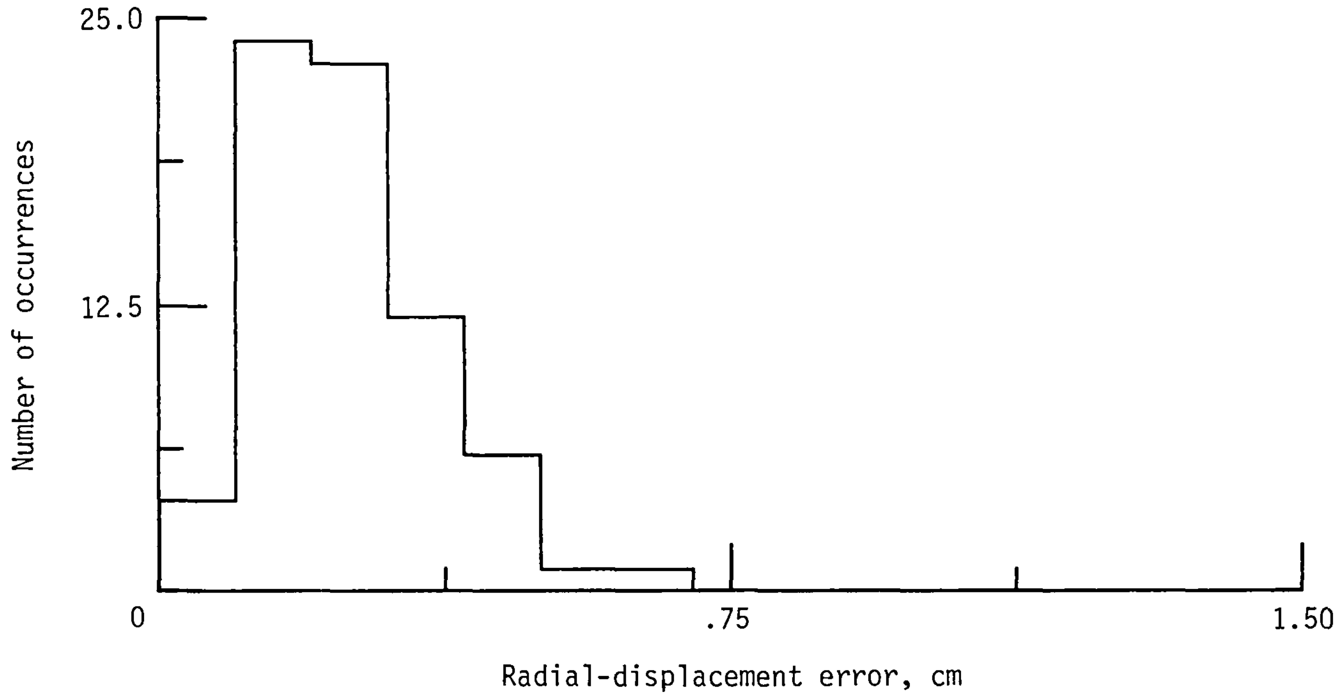

(d) Resolved-rate control. Proximity display on.

Figure 11.- Concluded.

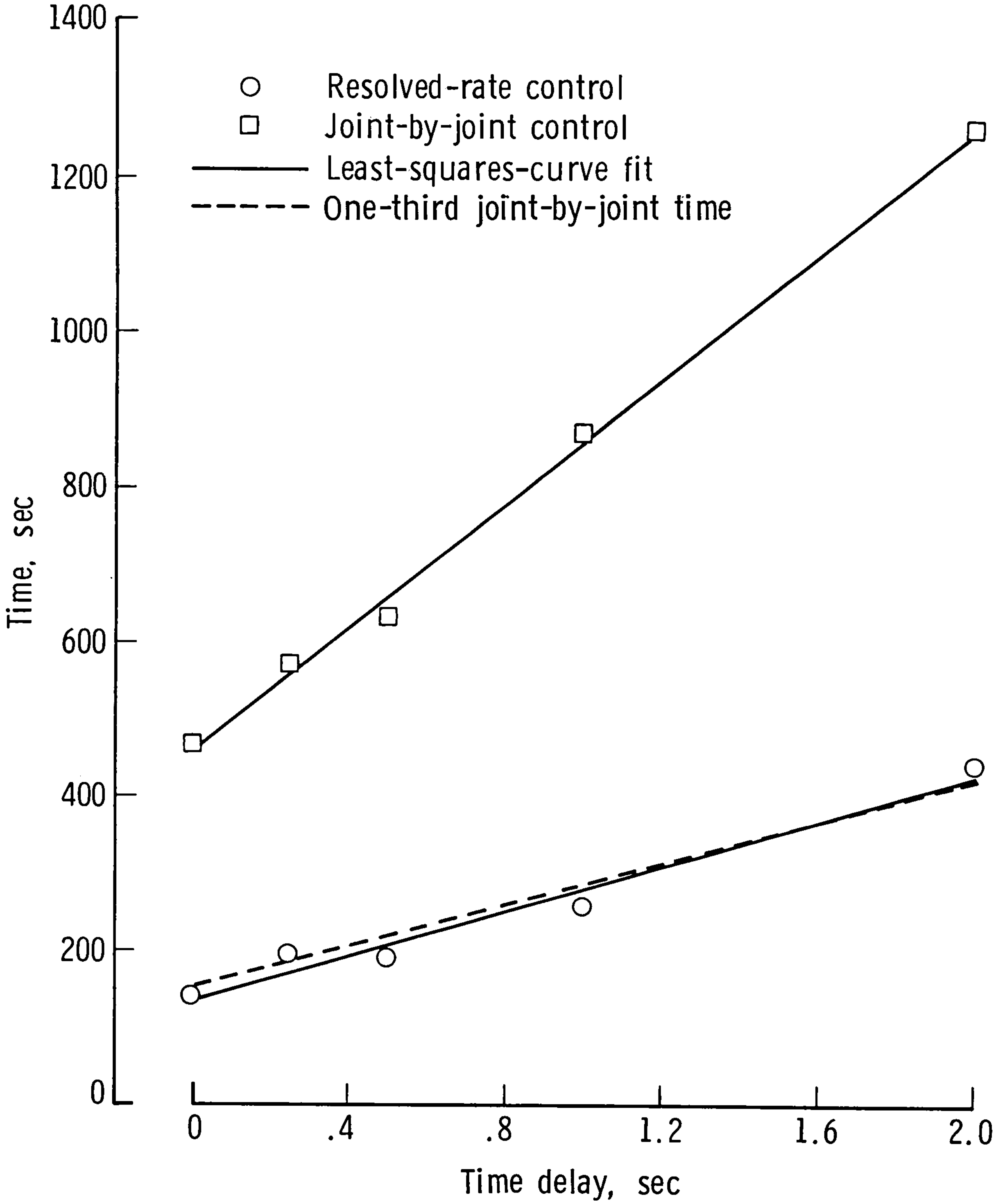

Figure 12.- Time required to complete task.

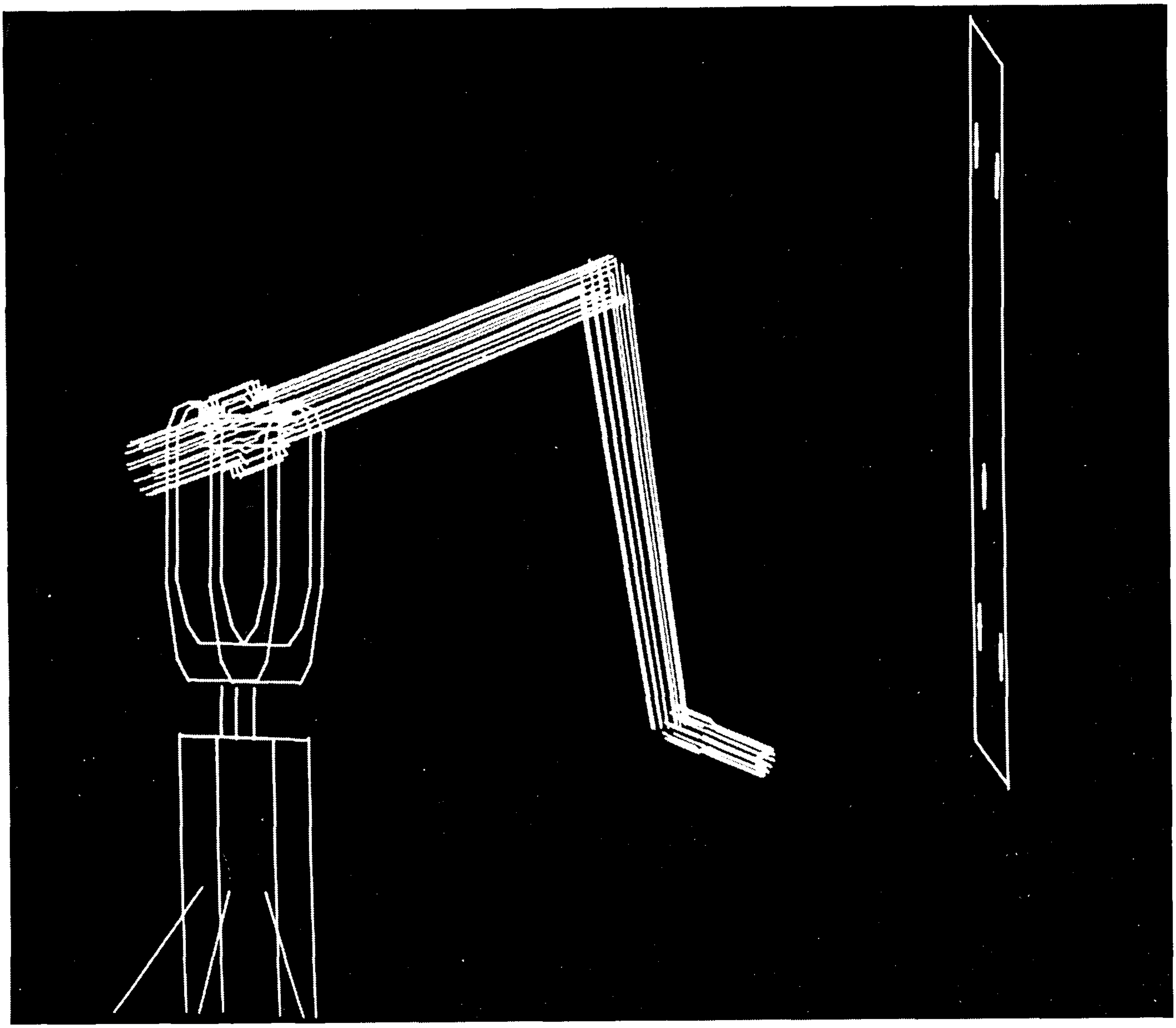

L-83-4247

(a) Camera at side of task board.

Figure 13.- View from initial simulated camera locations.

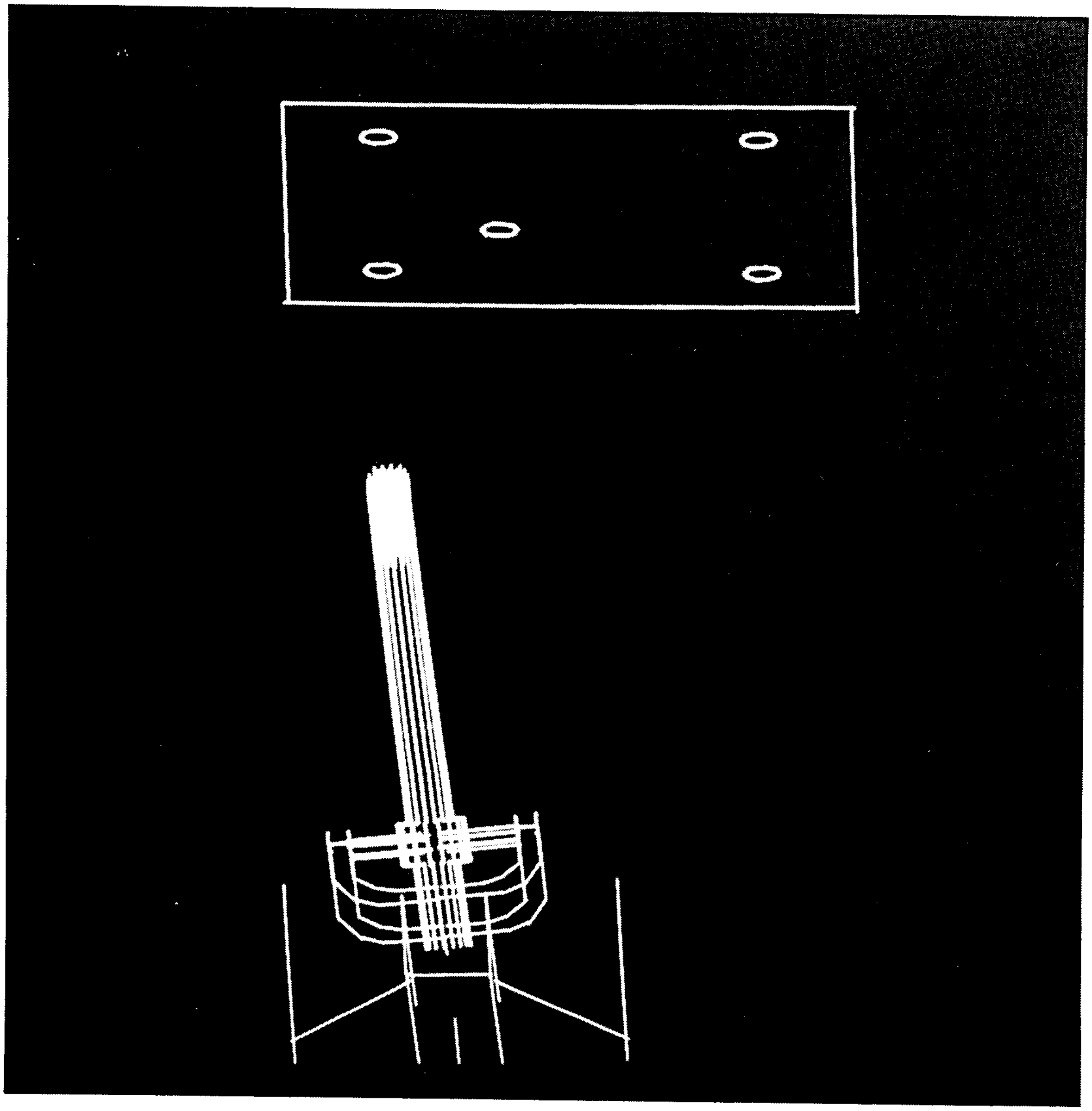

L-82-11,107

(b) Camera above task board.

Figure 13.- Concluded.

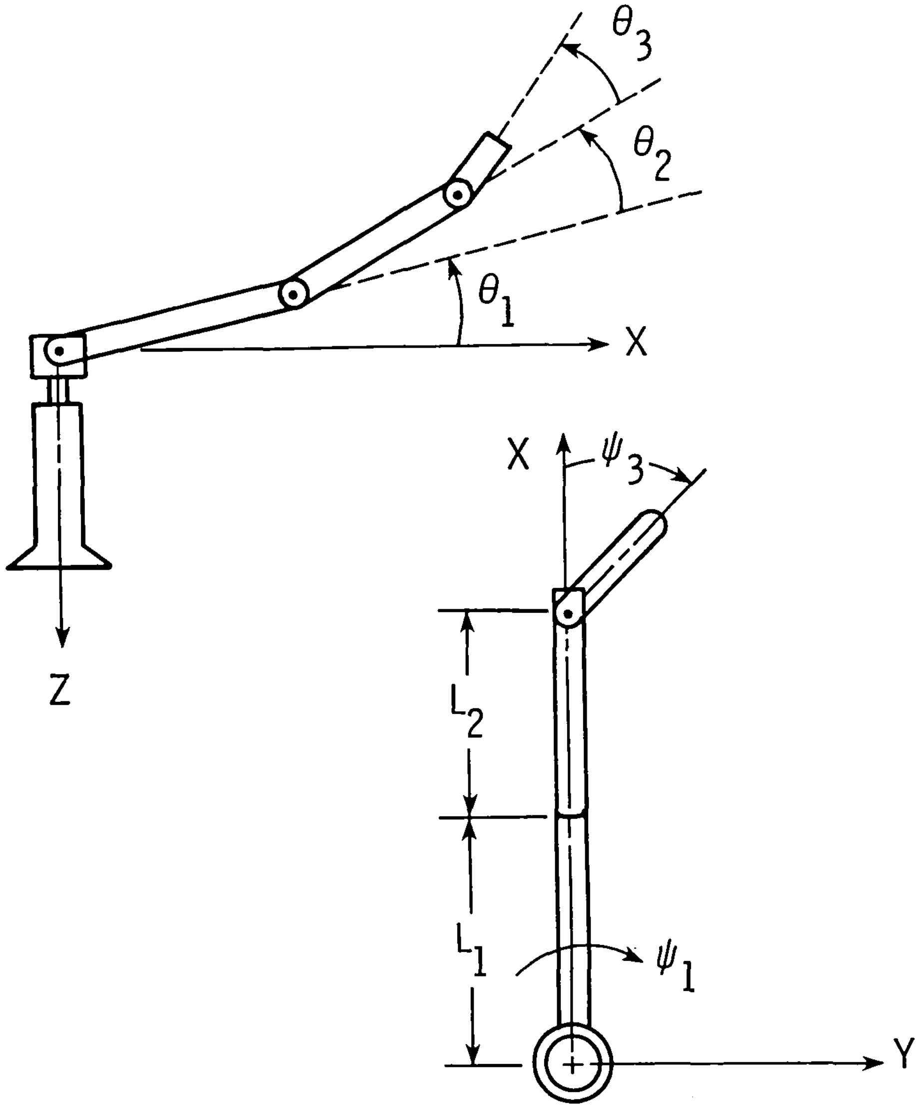

Figure 14.- Axis system used for resolved-rate equations.

1. Report No. NASA TM-85653	2. Government Accession No.	3. Recipient's Catalog No.
4. Title and Subtitle A RATE-CONTROLLED TELEOPERATOR TASK WITH SIMULATED TRANSPORT DELAYS		5. Report Date September 1983
		6. Performing Organization Code 506-64-23-01-00
7. Author(s) Jack E. Pennington		8. Performing Organization Report No. L-15561
9. Performing Organization Name and Address NASA Langley Research Center Hampton, VA 23665		10. Work Unit No.
		11. Contract or Grant No.
12. Sponsoring Agency Name and Address National Aeronautics and Space Administration Washington, DC 20546		13. Type of Report and Period Covered Technical Memorandum
		14. Sponsoring Agency Code
15. Supplementary Notes		

16. Abstract

A teleoperator-system simulation has been used to examine the effects of two control modes (joint-by-joint and resolved-rate), a proximity-display method, and time delays (up to 2 sec) on the control of a five-degree-of-freedom manipulator performing a probe-in-hole alignment task. Four subjects used proportional rotational control and discrete (on-off) translation control with computer-generated visual displays. The proximity display enabled subjects to separate rotational errors from displacement (translation) errors; thus, when the proximity display was used with resolved-rate control, the simulated task was trivial. The time required to perform the simulated task increased linearly with time delay, but time delays had no effect on alignment accuracy. Based on the results of this simulation, several future studies are recommended.

17. Key Words (Suggested by Author(s)) Teleoperator Simulation Time delay Proximity		18. Distribution Statement Unclassified - Unlimited Subject Category 54	
19. Security Classif. (of this report) Unclassified	20. Security Classif. (of this page) Unclassified	21. No. of Pages 45	22. Price A03

 NASA-Langley, 1983

National Aeronautics and
Space Administration

Washington, D.C.
20546

Official Business

Penalty for Private Use, $300

THIRD-CLASS BULK RATE

Postage and Fees Paid
National Aeronautics and
Space Administration
NASA-451

U.S.MAIL

NASA

POSTMASTER: If Undeliverable (Section 158 Postal Manual) Do Not Return